11 Characterization of Focal Liver Lesions

Emilio Quaia, Mirko D'Onofrio, Tommaso Vincenzo Bartolotta, Alessandro Palumbo, Massimo Midiri, Fabrizio Calliada, Sandro Rossi, and Roberto Pozzi Mucelli

CONTENTS

11.1 Introduction *125*
11.2 Scanning Technique for Focal Hepatic Lesions *126*
11.2.1 Preliminary Baseline Scan *126*
11.2.2 Scanning Modes After Microbubble Injection *127*
11.2.3 Dynamic Phases After Microbubble Injection *129*
11.2.4 Contrast Enhancement Patterns *132*
11.3 Benign Focal Liver Lesions *133*
11.3.1 Hemangioma *133*
11.3.2 Focal Nodular Hyperplasia *137*
11.3.3 Hepatocellular Adenoma *140*
11.3.4 Macroregenerative and Dysplastic Nodules *143*
11.3.5 Focal Fatty Sparing and Focal Fatty Changes *147*
11.3.6 Other Benign Focal Liver Lesions *148*
11.4 Malignant Focal Liver Lesions *151*
11.4.1 Hepatocellular Carcinoma *151*
11.4.2 Metastases *154*
11.4.3 Intrahepatic Cholangiocellular Carcinoma *158*
11.4.4 Other Malignant Focal Liver Lesions *158*
11.5 Clinical Results *159*
11.6 When Should Microbubble-Based Agents Be Employed? *160*
References *161*

E. Quaia, MD, Assistant Professor of Radiology;
A. Palumbo, MD
Department of Radiology, Cattinara Hospital, University of Trieste, Strada di Fiume 447, 34149 Trieste, Italy
R. Pozzi Mucelli, MD, Professor of Radiology;
M. D'Onofrio, MD, Assistant Professor of Radiology
Department of Radiology, Hospital GB Rossi, University of Verona, Piazza L.A. Scuro 10, 37134 Verona, Italy
T. V. Bartolotta, MD, Assistant Professor of Radiology;
M. Midiri, MD, Professor of Radiology,
Department of Radiology, University of Palermo, Via del Vespro 129, 90127 Palermo, Italy
F. Calliada, MD, Professor of Radiology
Department of Radiology, San Matteo Hospital, University of Pavia, Piazzale Golgi 1, 27100 Pavia, Italy
S. Rossi, MD
Operative Unit for Interventional US, San Matteo Hospital, University of Pavia, Piazzale Golgi 1, 27100 Pavia, Italy

11.1 Introduction

Focal liver lesions may be identified incidentally, e.g., during an abdominal ultrasound (US) scan performed for clinical reasons unrelated to the liver lesion or during staging or follow-up procedures for a primary neoplasm or liver cirrhosis. Focal liver lesions may be characterized by baseline gray-scale US and color Doppler US when a typical pattern is identified, as in the case of homogeneously hyperechoic hemangiomas (Vilgrain et al. 2000) or focal nodular hyperplasia with a spoke-wheel shaped central vascular pattern on color Doppler US (Wang et al. 1997). Even though color Doppler US may improve diagnostic confidence in the characterization of focal liver lesions (Taylor et al. 1987; Hosten et al. 1999a; Tanaka et al. 1990; Nino-Murcia et al. 1992; Numata et al. 1993; Reinhold et al. 1995; Lee et al. 1996; Gonzalez-Anon et al. 1999), it does have important limitations since benign and malignant lesions may show a similar appearance on both gray-scale and color Doppler US.

It has been shown that the visibility of peripheral and intratumoral vessels may be improved on color and power Doppler US after the injection of microbubble-based contrast agents (Hosten et al. 1999b; Kim et al. 1999; Lee et al. 2002; Leen et al. 2002). Nevertheless, color signal saturation, motion and blooming artifacts, insensitivity to the flow of capillary vessels and limited sensitivity to the signal produced by microbubble-based agents represent important limitations of color Doppler US.

Microbubble-based contrast agents (Gramiak and Shah 1968) and dedicated US contrast-specific modes were introduced to overcome the limitations of baseline gray-scale and color Doppler US. Air-, perfluorocarbon- or sulfur hexafluoride-filled microbubbles may be employed to characterize focal liver lesions, though the technique of scanning differs according to the employed agent.

Levovist (SH U 508A, Schering, Berlin, Germany) is an air-filled microbubble contrast agent covered by

a shell of galactose and palmitic acid. Since Levovist presents a low acoustic nonlinear response and low production of harmonic frequencies when insonated at a low acoustic transmit power, insonation with high acoustic power is necessary to produce microbubble destruction with emission of a wideband frequency signal detectable by dedicated contrast-specific techniques. Destructive imaging requires intermittent scanning and a limited number of sweeps to minimize bubble rupture and, consequently, does not allow prolonged evaluation of liver contrast enhancement. In comparison with baseline US, the injection of Levovist has been shown to allow the identification of tumoral vessels, to differentiate benign and malignant focal liver lesions according to the enhancement pattern (Bertolotto et al. 2000; Burns et al. 2000; Kim TK et al. 2000; Wilson et al. 2000; Blomley et al. 2001; Numata et al. 2001; Dill-Macky et al. 2002; von Herbay et al. 2002; Kim EA et al. 2003; Migaleddu et al. 2004; Wen et al. 2004), and to improve the characterization of focal liver lesions in terms of both overall accuracy and diagnostic confidence (Tanaka et al. 2001; Isozaki et al. 2003; von Herbay et al. 2002; Bryant et al. 2004). The late liver-specific phase of Levovist (Blomley et al. 1998, 1999; Quaia et al. 2002b), beginning from 3 to 5 min after injection, has been demonstrated to be the most important dynamic phase for the characterization of focal liver lesions (Blomley et al. 2001; Bryant et al. 2004). During the late phase, benign liver lesions present similar microbubble uptake to the adjacent liver, while malignant liver lesions present lower microbubble uptake (Bertolotto et al. 2000; Burns et al. 2000; Blomley et al. 2001; Bryant et al. 2004).

New generation perfluorocarbon- or sulfur hexafluoride-filled microbubbles covered by a phospholipid shell, such as SonoVue (BR1, Bracco, Milan, Italy), Definity (MRX 115, Bristol-Myers Squibb, North Billerica, MA, NY, USA), and Sonazoid (NC100100, Nycomed Amersham, Oslo, Norway), present a nonlinear response with production of harmonic and subharmonic frequencies (Schneider et al. 1995; Morel et al. 2000; Correas et al. 2000, 2001; Cosgrove et al. 2002) at low acoustic power insonation, allowing the employment of nondestructive imaging and the real-time evaluation of contrast enhancement in focal liver lesions (Albrecht et al. 2003; Brannigan et al. 2004; Nicolau et al. 2003a; Hohmann et al. 2003; Quaia et al. 2004). Preliminary experimental and clinical investigations proved the safety and efficacy of SonoVue in vascular and parenchymal diagnostic applications (Quaia et al. 2003, 2004).

Besides commercial microbubble-based contrast agents, direct intra-arterial CO_2 injection into the proper hepatic artery after selective hepatic arteriography and superior mesenteric arteriography has been proposed for the assessment of vascularity in hepatic tumors and particularly in hepatocellular carcinoma (Chen et al. 2002; Kudo et al. 1992).

11.2 Scanning Technique for Focal Hepatic Lesions

11.2.1 Preliminary Baseline Scan

Before microbubble injection, sonologists must perform a complete and accurate assessment of the liver parenchyma and of each identified focal liver lesion. The baseline scan includes the assessment of lesion appearance on gray-scale and color Doppler US, with the employment of tissue harmonic imaging and compound imaging (Claudon et al. 2002) and of state-of-the-art US equipment provided by wideband frequency transducers. Although tissue harmonic imaging was originally developed for microbubble-based contrast agents(Burns et al. 1996; Ward et al. 1997), it also allows a clear enhancement of the image quality in native tissues. This is achieved by improvement of contrast resolution, particularly in patients who are difficult to image with conventional techniques, by reduction of the artifacts that degrade conventional sonograms, and by improvement in the differentiation between solid and liquid components. Compound imaging may combine multiple coronal images obtained from different spatial orientations, i.e., spatial compound imaging (Jespersen et al. 1998), or may involve the acquisition of images of the same object at different frequencies, combining them into a single image, i.e., frequency compound imaging (Gatenby et al. 1989). The result is the generation of a single image with better delineated margins and curved surfaces, fewer image artifacts, speckles (echoes from subresonation scatterers), and noise, and improved image contrast.

Baseline color Doppler US is performed by using slow-flow settings (pulse repetition frequency 800–1,500 Hz, wall filter of 50 Hz, high levels of color versus echo priority, and color persistence). Color gain is varied dynamically during the examination to enhance color signals and avoid excessive noise, with the size of the color box being adjusted

to include the entire lesion in the field of view of the color image. Spectral analysis of central and peripheral vessels is performed by pulsed Doppler to reveal continuous venous or pulsatile arterial flows.

11.2.2 Scanning Modes After Microbubble Injection

Two different insonation modes, destructive and nondestructive, may be employed after microbubble injection according to the acoustic power output, which is related to the employed mechanical index (MI) value. The MI value is a practical index to express the intensity of the acoustic field, even though it is an unreliable predictor of microbubble destruction, since the same MI value corresponds to different powers of the transmitted US beam in different US systems (Merritt et al. 2000). The destructive mode has to be performed using the highest available MI to achieve extensive bubble rupture and production of a wideband frequency signal.

a) Destructive high acoustic power intermittent mode. This technique employs high acoustic power insonation to achieve microbubble destruction with emission of a transitory broadband frequency signal. It is suitable for agents with a late liver-specific postvascular phase, such as Levovist (Blomley et al. 1998, 2001; Quaia et al. 2002b) and Sonavist (SH U563 A, Schering AG, Berlin, Germany), because it allows effective assessment and characterization of focal liver lesions during the late phase: malignant liver lesions typically do not retain microbubbles while benign lesions present persistent microbubble uptake (Blomley et al. 1998; Bryant et al. 2004). To minimize microbubble rupture, destructive imaging requires intermittent scanning and a limited number of sweeps. Moreover, the high acoustic power of insonation produces a marked mixture of tissue harmonics and microbubble harmonics (Cosgrove et al. 2002), with production of a significant tissue background on which the bubble signal is superimposed.

Intermittent scanning may be manually or ECG triggered or it may be turned on simply by defreez-

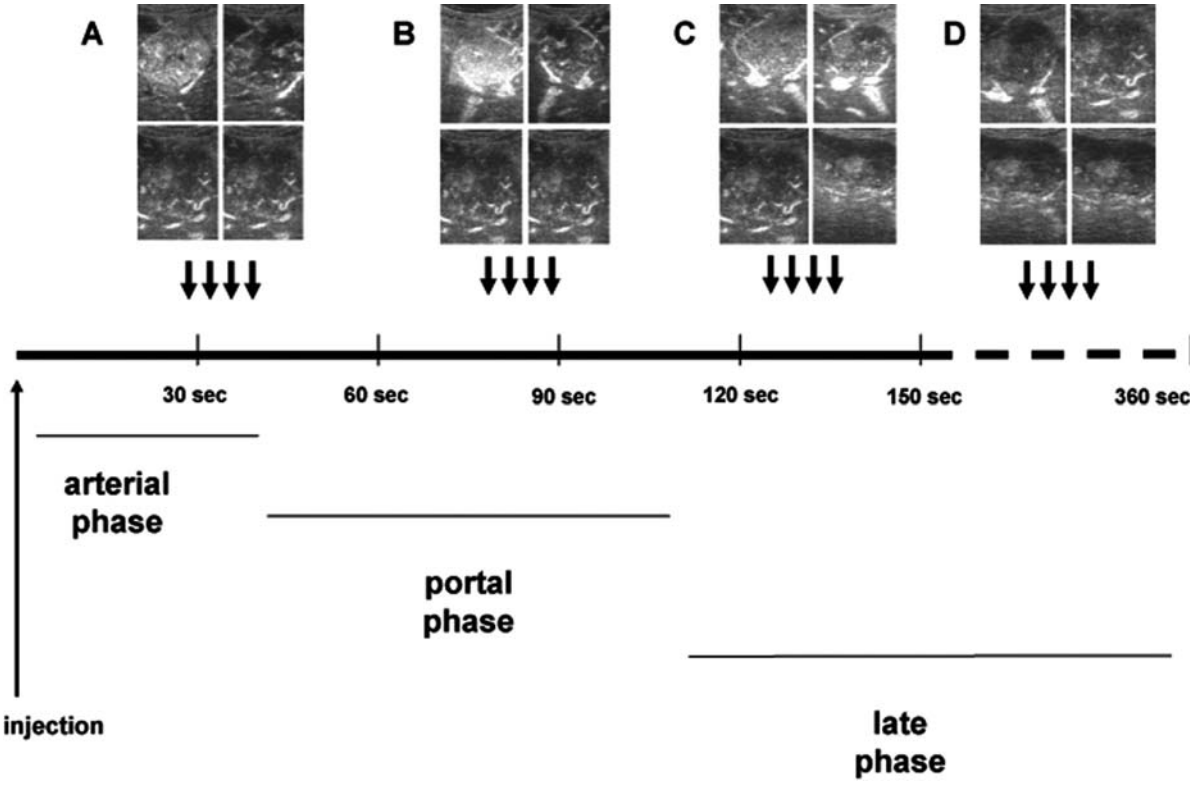

Fig. 11.1. Scheme of intermittent high acoustic power insonation for the characterization of focal liver lesions. Different trains of four high acoustic power US pulses are sent during the arterial, portal, and late phases. During the arterial phase, which is brief, a single train is transmitted. During the portal and late phases, which are longer than the arterial phase, two trains for each phase may be transmitted.

ing imaging for 1–2 s. Different trains with four to six high acoustic power US pulses may be employed (Fig. 11.1). The gray-scale gain is set immediately below the noise threshold, with one focal zone positioned just below the lesion. The delay time between the first and second destructive pulses of each train, corresponding to 110–140 ms (0.110–0.140 s = 1/frame rate = 1/7–1/9), is long enough to allow bubble refilling in large tumor vessels with fast flow but too brief to allow refilling in tumoral capillary and microvessels with slow flows. Since bubbles are rapidly destroyed from the first to the second frame, altering image contrast from a fractional blood volume-weighted image (first frame, Fig. 11.2) to a fractional blood flow-weighted image (second and subsequent frames, Fig. 11.2), the first frame represents both large and small tumor vessels and shows the pattern of contrast enhancement, while the second frame selectively represents large arterial/venous vessels with fast flow and permits assessment of tumor vessel appearance and distribution. The following two frames obtained from each train do not add any significant findings; they appear very similar to the second frame and are characterized only by a progressive reduction in bubble content due to bubble rupture.

b) Nondestructive low acoustic power continuous mode. This mode of insonation was allowed by the introduction of a new generation of perfluorocarbon- or sulfur hexafluoride-filled microbubbles and of multipulse scanning modes showing increased sensitivity to the nonlinear harmonic responses of the microbubbles and more effective suppression of tissue signals. A frequency corresponding to the microbubble resonance frequency is transmitted, and

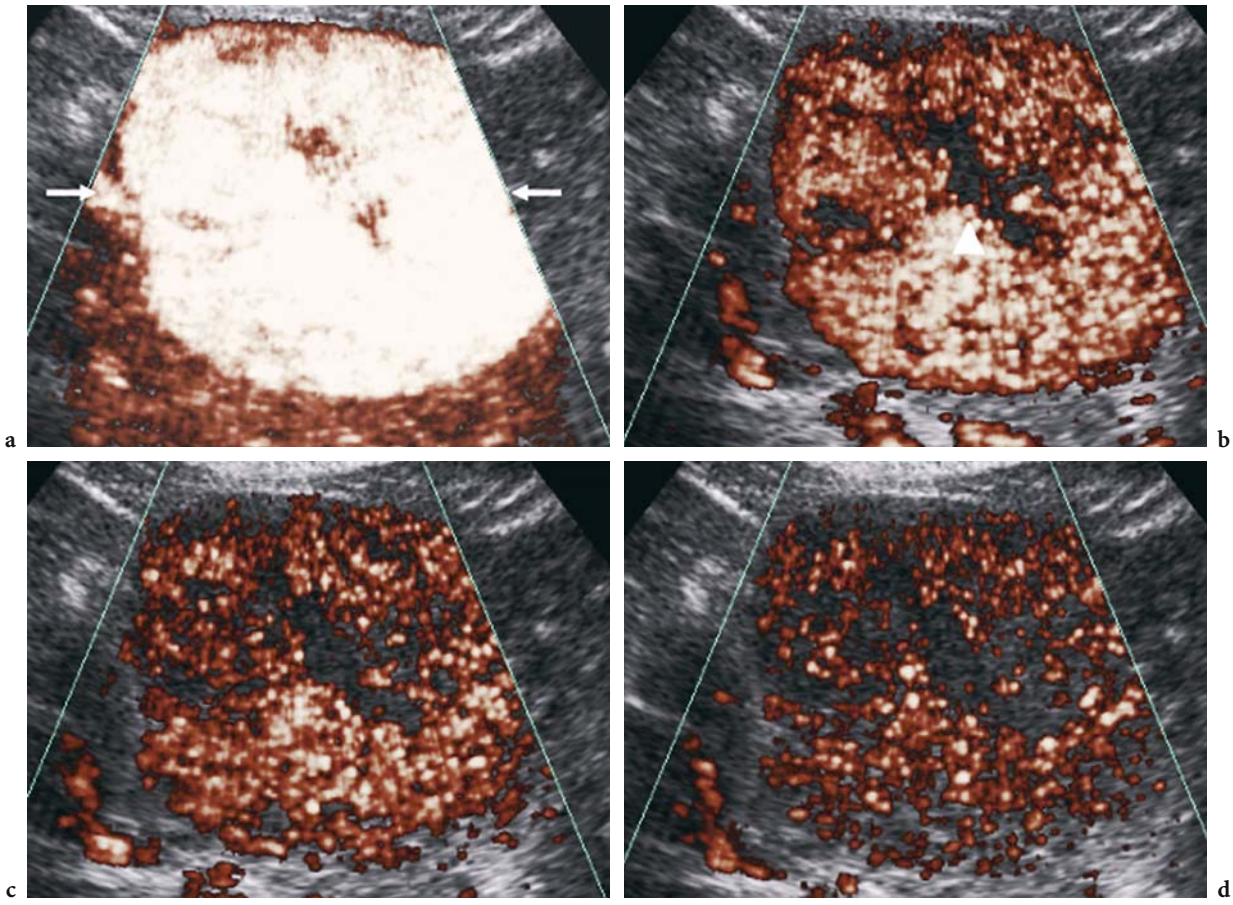

Fig. 11.2a–d. Stimulated acoustic emission after air-filled microbubble injection at high acoustic power insonation. Agent Detection Imaging (Philips-ATL, WA, USA). Four frames were obtained from high transmit power insonation. Diffuse contrast enhancement (*arrows*) is evident in the late phase (**a**) in the first frame of the train. In the subsequent frames of the train (**b–d**), contrast enhancement decreases progressively due to microbubble destruction, with evidence of a central scar spared by contrast enhancement.

harmonic frequencies are generated from nonlinear behavior of microbubbles (Cosgrove et al. 2002). Harmonic frequencies that present a value double that of the fundamental frequency may be detected by using dedicated contrast-specific imaging modes.

The nondestructive mode has several advantages over the destructive mode. First, it allows the effective suppression of tissue background signal since the stationary native tissue does not produce harmonic signals when insonated at low acoustic power. Second, the nondestructive mode allows assessment of contrast enhancement in real time, avoiding scan delay; it even offers better temporal resolution than contrast-enhanced CT and MR imaging. Third, this technique permits the acoustic window to be changed after microbubble injection. Possible disadvantages of nondestructive as compared with destructive imaging are a lower signal-to-noise ratio and the narrower dynamic range caused by the lower acoustic power of insonation.

Insonation should encompass all the arterial phase and must be extended to the first part (20 s) of the portal phase (Fig. 11.3). During the following seconds of the portal phase and during the late phase, the sonologist should perform brief insonations of 5–10 s and then resume the contrast-specific mode for 20–30 s to allow lesion replenishment by microbubbles (Fig. 11.3). These brief insonations should number at least two for the portal phase and three for the late phase. During the late phase each lesion should be scanned up to microbubble disappearance from the microcircle (6–8 min).

11.2.3 Dynamic Phases After Microbubble Injection

Different dynamic phases of contrast enhancement may be identified in the liver parenchyma after the injection of microbubble-based contrast agents, as for computed tomography (CT) or magnetic resonance (MR) imaging after the injection of iodinated or paramagnetic agents (van Leeuwen et al. 1996),

The arterial (vascular) phase is very brief. It begins at about 10–20 s after microbubble injection (Figs. 11.4a, 5a–d) and lasts up to 25–35 s from the

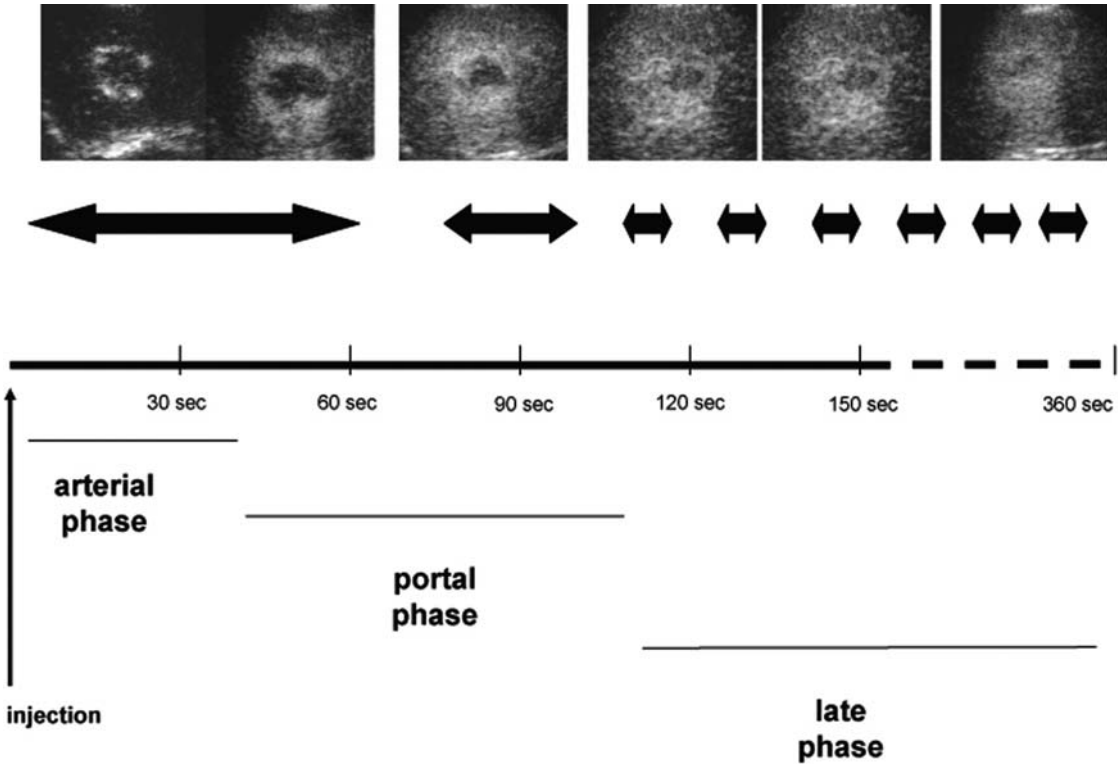

Fig. 11.3. Scheme of continuous low acoustic power mode insonation for the characterization of focal liver lesions. A single continuous scan has to be performed during the arterial phase, while several brief scans may be employed during the portal and late phases. For the latter purpose, insonations of 5–10 s are performed, with subsequent resumption of the contrast-specific mode for 20–30 s

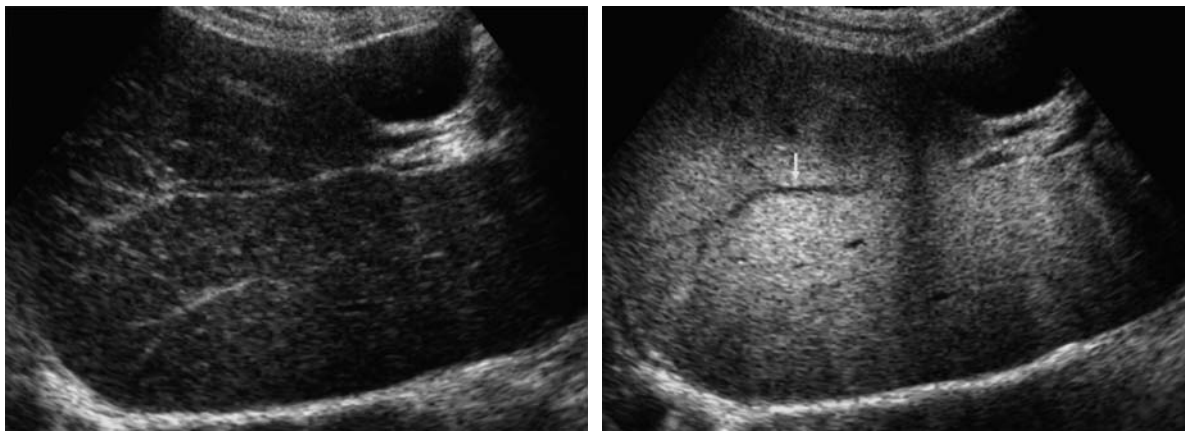

Fig. 11.4a,b. Transverse scan. Appearance of the liver during the arterial (**a**) and late (**b**) phases after Levovist (air-filled microbubble agent) injection at high acoustic power insonation. Intense contrast enhancement is demonstrated during the late liver-specific phase (**b**) 5 min after microbubble injection) owing to microbubble destruction. During the late liver-specific phase, microbubbles are pooling in liver sinusoids without evidence of microbubbles in the portal vessels (*arrow*), which appear as voids in the diffusely enhancing liver parenchyma.

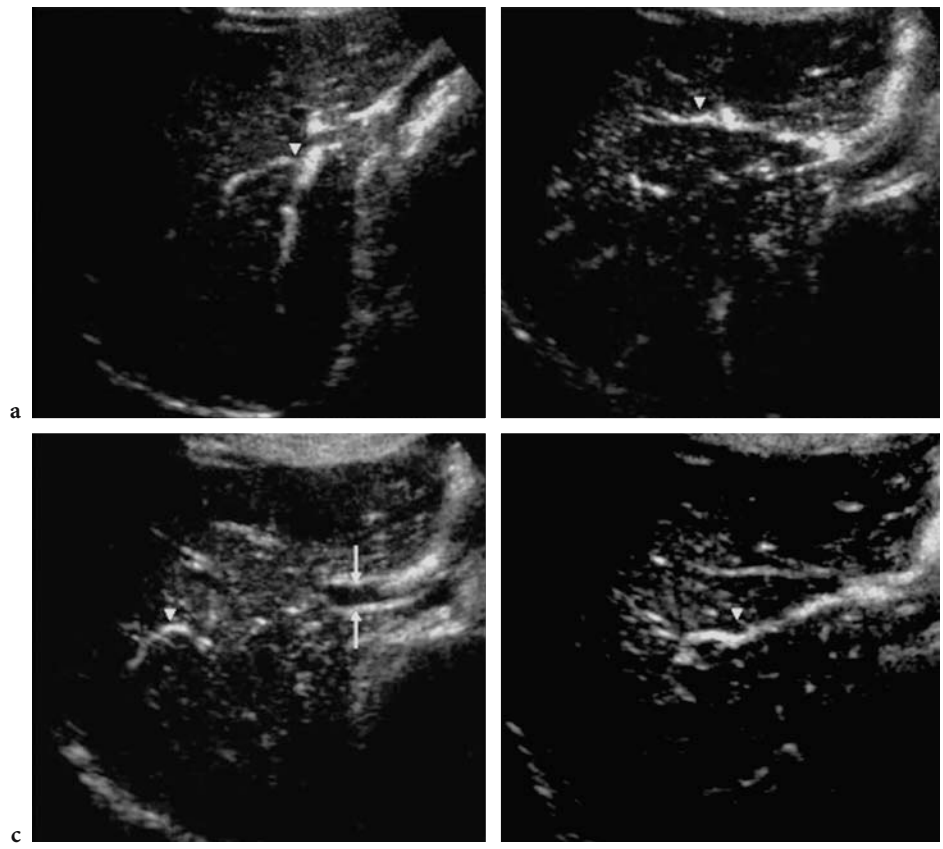

Fig. 11.5a–l. Longitudinal scan. Appearance of the liver during the arterial (**a–d**), portal (**e–h**), and late (**i–n**) phases after SonoVue (sulfur hexafluoride-filled microbubble agent) injection at low acoustic power insonation. During the arterial phase (**a–d**), 15 s after microbubble injection, microbubbles fill the hepatic arterial vessels (*arrowheads*), sparing the portal vein (*arrows*) and portal intrahepatic vessels. During the portal phase (**e–h**), 45 s after microbubble injection, microbubbles fill the portal vessels (*arrows*), progressively filling the liver sinusoids. In the late phase (**i–l**), 120 s after microbubble injection, microbubbles fill the liver sinusoids, giving rise to diffuse contrast enhancement in the liver parenchyma.

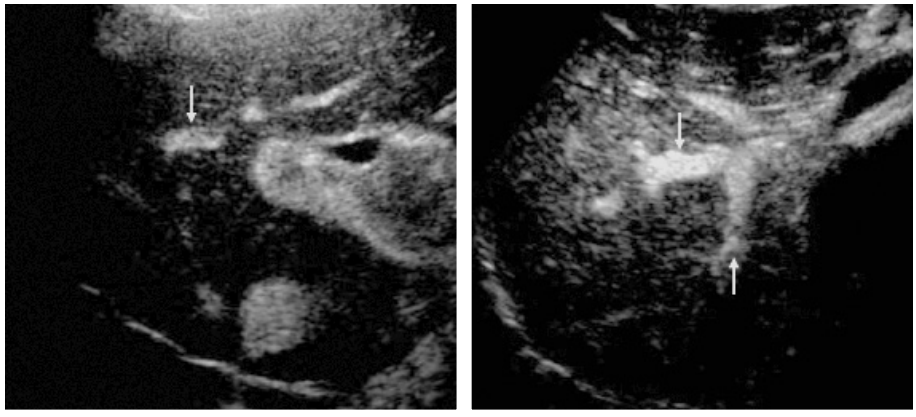

e f

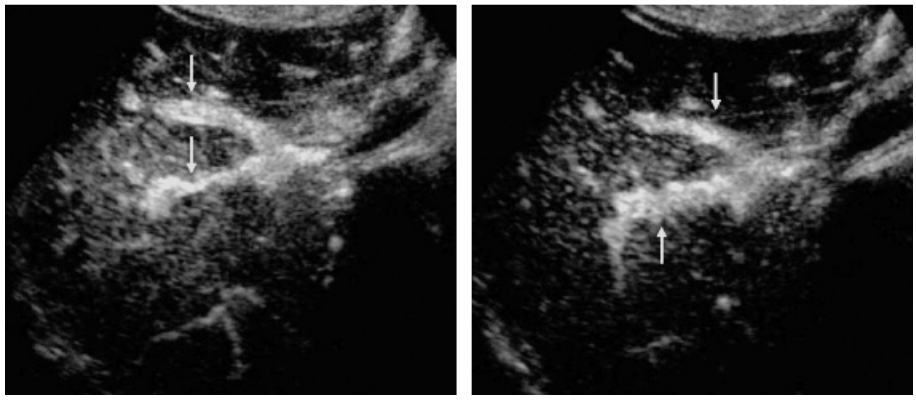

g h

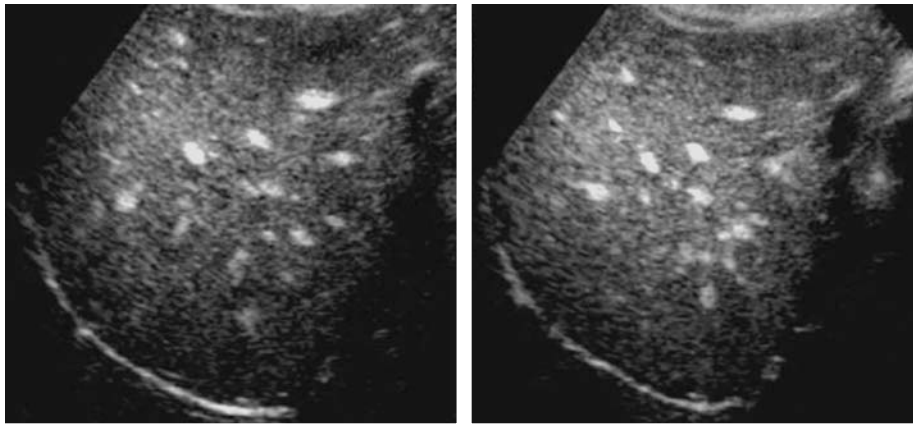

i j

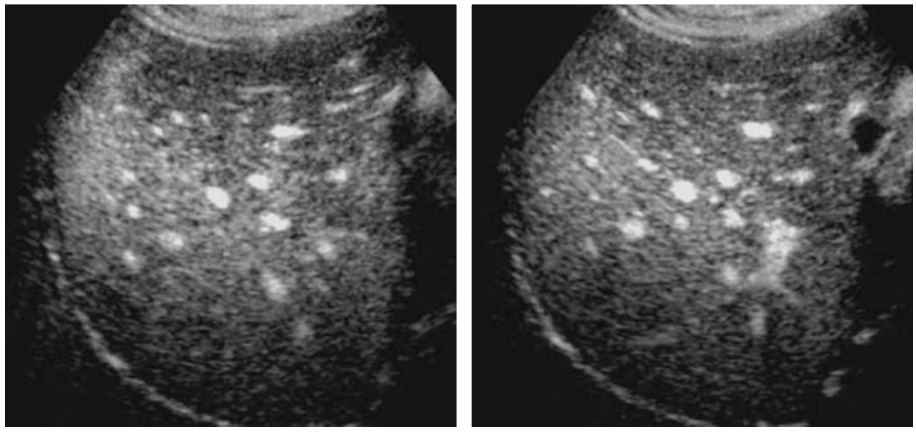

k l

time of injection according to the circulation time (Albrecht et al. 2003; Lee et al. 2003). The arterial phase is necessary to evaluate lesion perfusion: diffuse and intense contrast enhancement is observed in hypervascular focal liver lesions whereas hypovascular focal liver lesions are characterized by absent or dotted contrast enhancement.

The portal and late phases (Figs. 11.4b, 11.5e–n) are much longer. The portal phase begins at 30–35 s and lasts up to 100–110 s from the beginning of microbubble injection. In liver cirrhosis, altered hepatic blood flow dynamics are frequently found, resulting in increased arterial flow and decreased portal vein flow to the liver (Quiroga et al. 2001). Therefore, patients with advanced cirrhosis often have inadequate, and sometimes transient, hepatic parenchymal enhancement during the portal phase (Chen et al. 1999). It is likely that in CT and MR imaging the portal phase has limited usefulness for the characterization of hepatic neoplasms.

The late (delayed or parenchymal) phase begins after the portal phase and lasts about 5–8 min, up to the time of disappearance of the microbubbles from the peripheral circulation. The late phase of microbubble agents is different from the equilibrium phase of non-liver-specific CT and MR contrast agents, since microbubble-based contrast agents do not present an interstitial (equilibrium or postvascular) phase and are pure intravascular agents. For this reason, microbubbles circulate in liver sinusoids during the late phase and different agents display different persistence in sinusoids.

After blood pool clearance, air-filled agents, such as Levovist or Sonavist, and perfluorocarbon-filled agents, such as Sonazoid (NC100100, Amersham Health, Oslo, Norway), have also been demonstrated to show hepatosplenic-specific parenchymal affinity in the late phase, during which the microbubbles are stationary in liver and spleen, in part pooled in sinusoids and in part phagocytosed by the reticuloendothelial system (Hauff et al. 1997; Blomley et al. 1998; Quaia et al. 2002a; Kindberg et al. 2003). This phase is comparable to the late phase of liver-specific MR agents such as gadobenate dimeglumine (Gd-BOPTA; Multihance; Bracco Imaging, Milan, Italy).

The late phase, with or without liver specificity, has been shown to be the most important for the characterization of focal liver lesions since benign lesions typically present persistent microbubble uptake with a hyper- or isovascular appearance relative to the adjacent liver while malignant lesions typically display microbubble washout with a hypovascular appearance (Blomley et al. 2001; Albrecht et al. 2003; Nicolau et al. 2003a,b; Bryant et al. 2004; Quaia et al. 2004). For these reasons, the late phase is the most important in the characterization of focal liver lesions, as with liver-specific MR agents (Grazioli et al. 2001a,b).

11.2.4 Contrast Enhancement Patterns

The echogenicity of focal liver lesions on baseline gray-scale US and the tumoral vascularity and staining after microbubble-based contrast agent injection have to be compared with the adjacent liver. Lesions with a homogeneous or slightly heterogeneous echo intensity distribution are defined as hyper-, iso-, or hypoechoic (or hyper-, iso-, or hypovascular), depending on whether they display a prevalently higher, similar, or lower echogenicity relative to the adjacent liver parenchyma. In all other cases, lesions are defined as heterogeneous.

According to the lesion appearance during the arterial phase, contrast enhancement patterns (Fig. 11.6) are classified as: (a) absent (no difference before and after microbubble injection), (b) dotted (tiny separate spots of enhancement distributed throughout the lesion), (c) rim-like (continuous ring of peripheral contrast enhancement), (d) nodular (discontinuous or continuous peripheral enhancement with nodular appearance), (e) central (enhancement of the central portion of the lesion, defined as spoke-wheel shaped if the central vessel appears to branch toward the periphery of the lesion), or diffuse (enhancement of the whole lesion) with either (f) a homogeneous or (g) a heterogeneous appearance.

It has been proposed (Tanaka et al. 2001), the diffuse heterogeneous enhancement in hepatocellular carcinomas should be defined as mosaic-like if only some parts of the tumor show enhancement during the arterial phase and reticular if net-like enhancement appears throughout the tumor during the portal and late phases.

According to the lesion appearance during the late phase, contrast enhancement patterns (Fig. 11.7) are classified as: (h) hypoechoic (compared to the echogenicity of adjacent liver parenchyma), (i) residual (central hypoechoic area in a lesion with a persistent hyper- or isoechoic appearance), (l) hyperechoic (compared to the echogenicity of adjacent liver parenchyma), or (m) heterogeneous (prevalently hypoechoic or hyperechoic).

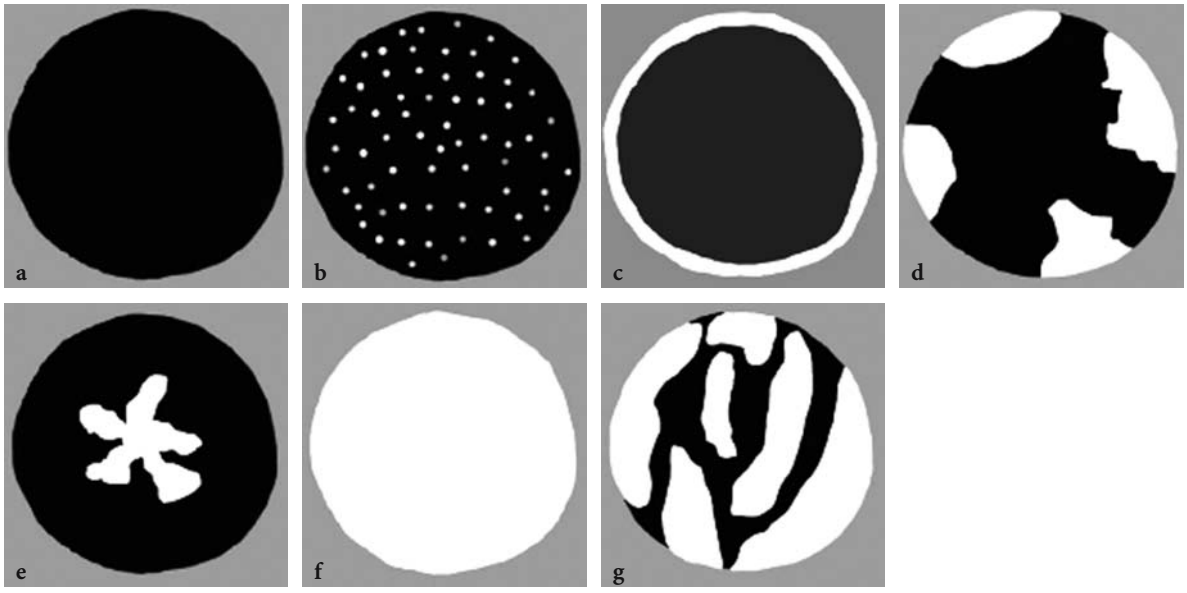

Fig. 11.6a–g. The different patterns of contrast enhancement in focal liver lesions during the arterial phase: **a** absent, **b** dotted, **c** peripheral rim-like, **d** peripheral nodular, **e** central with a spoke-wheel shape, **f** diffuse homogeneous, **g** diffuse heterogeneous.

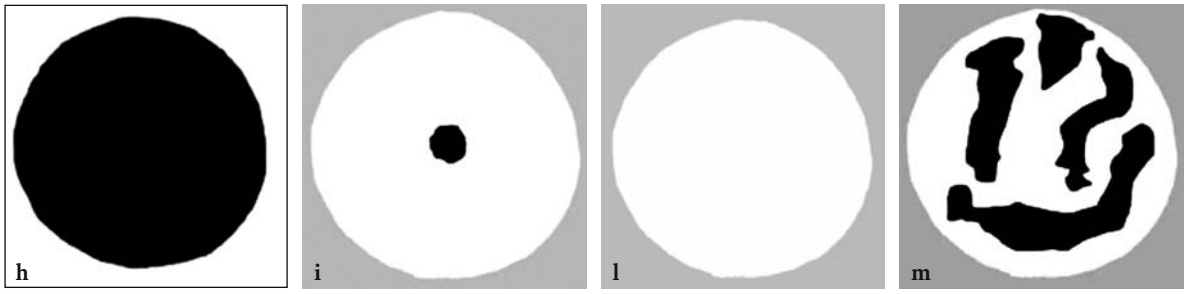

Fig. 11.7h–m. The different patterns of contrast enhancement in focal liver lesions during the late phase: **h** hypoechoic (or hypovascular), **i** residual central hypoechoic area in a lesion with a persistent iso- to hyperechoic (or iso- to hypervascular) appearance, **l** hyperechoic (hypervascular), **m** heterogeneous.

11.3 Benign Focal Liver Lesions

11.3.1 Hemangioma

Epidemiology and histopathologic features. Hemangiomas are the most common benign tumors of the liver (Ros 1990), with an incidence in the general population ranging from 0.4% to 20% (Edmondson 1958; Karhunen 1986). Although hemangiomas occur more frequently in women, they are not particularly prevalent at any age. Hemangiomas show an association with focal nodular hyperplasia, and the two lesions may coexist in the same liver (Vilgrain et al. 2003).

Multimodality imaging - US and color Doppler US. Liver hemangiomas may display a typical appearance on baseline gray-scale US consisting in a hyperechoic and homogeneous or centrally heterogeneous pattern, with or without posterior acoustic enhancement and well-defined regular margins (Vilgrain et al. 2000). Besides their typical appearance, liver hemangiomas may also present atypical and therefore indeterminate patterns on baseline US, appearing either homogeneous or heterogeneous, hypoechoic or isoechoic, and with or without a thin peripheral echoic border (Vilgrain et al. 2000; Quaia et al. 2002a). Even though typical liver hemangiomas do not need further confirmatory studies, both benign (focal fatty change, hepatocellular adenoma, focal nodular hyperplasia, lipoma) and malignant (hepato-

cellular carcinoma and metastasis) focal liver lesions may present a similar appearance to hemangiomas on baseline gray-scale US. Like baseline gray-scale US, color Doppler US shows only moderate accuracy in the characterization of liver hemangiomas and may also be limited by motion artifacts and low sensitivity to slow flows. Absence of flow or a small number of intratumoral color spots may be observed in smaller hemangiomas, while intratumoral vessels, mostly with a venous flow, are seen in larger hemangiomas (Quaia et al. 2002a).

Multimodality imaging – CT and MR imaging. The imaging procedures most frequently employed to characterize liver hemangiomas are CT and MR imaging, performed after contrast agent administration during different dynamic phases (arterial, portal, equilibrium, and late phases). The typical contrast enhancement pattern of hemangiomas consists in peripheral nodular enhancement with progressive centripetal fill-in (Nino-Murcia et al. 2000). Nevertheless, a variety of less frequent or less typical contrast enhancement patterns may be observed, such as diffuse contrast enhancement in hypervascular hemangiomas or absence of contrast enhancement in fibrotic hemangiomas, which are frequently detected in cirrhotic patients (Brancatelli et al. 2001a).

Contrast-enhanced US. Various contrast enhancement patterns may be observed in liver hemangiomas after the administration of microbubble-based contrast agents.

Most liver hemangiomas display peripheral nodular enhancement (Fig. 11.8) during the arterial

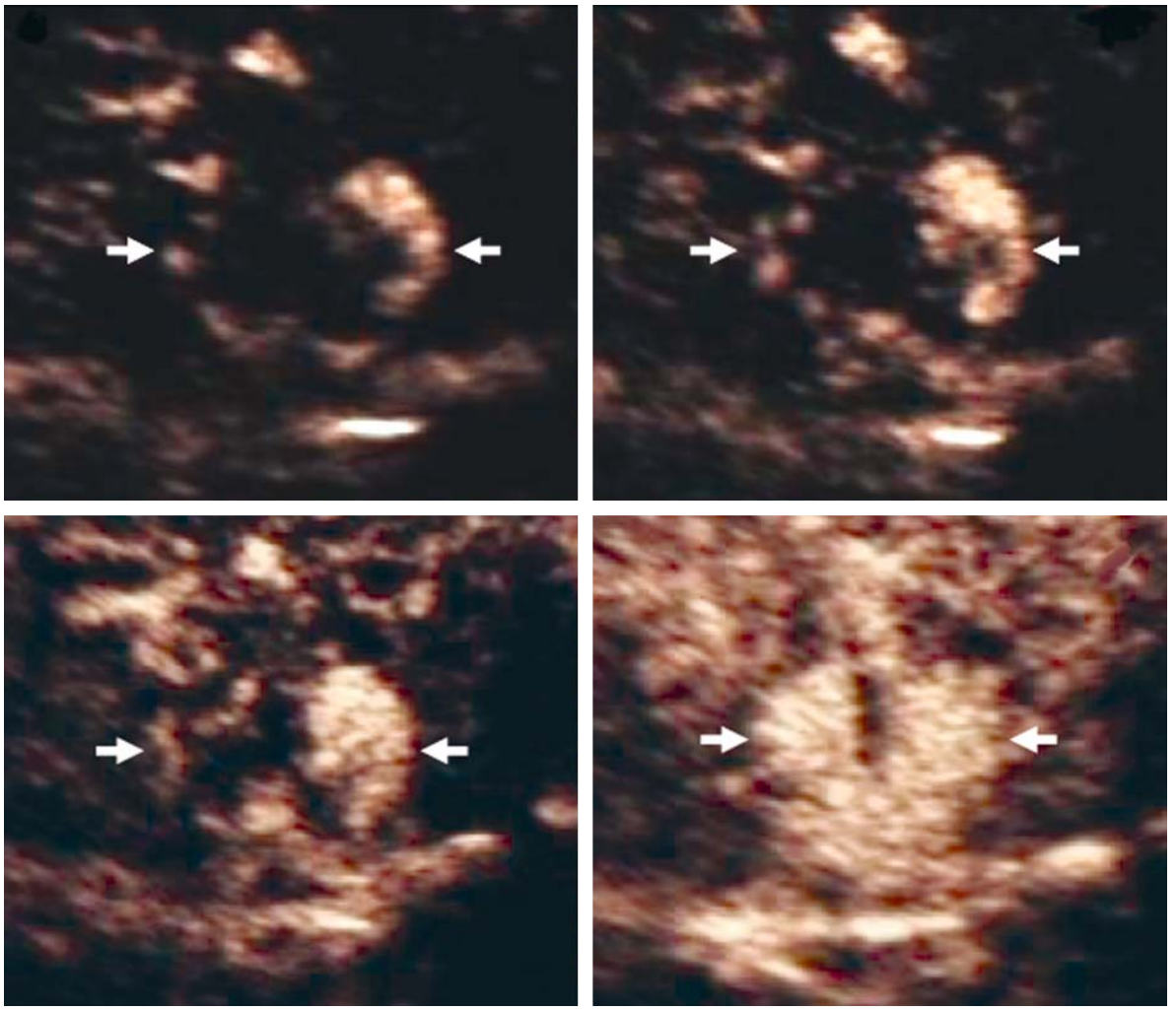

Fig. 11.8a–d. Hemangioma: typical peripheral nodular contrast enhancement pattern with progressive fill-in. Contrast-specific mode: Cadence Contrast Pulse Sequence (Siemens-Acuson, CA, USA) with low acoustic power insonation. Peripheral nodular enhancement is demonstrated during the arterial phase (**a**), with progressive centripetal fill-in during the portal (**b, c**) and late (**d**) phases.

phase, with progressive centripetal fill-in from 50 to 280 s after injection. During the late phase, the centripetal fill-in appears complete in 40–50% of cases (Lee et al. 2002; Nicolau et al. 2003a), and partial in the remainder (owing to the presence of intratumoral areas of fibrosis or thrombosis).

Hyperechoic liver hemangiomas may also show progressive fill-in without evidence of centripetal progression (Fig. 11.9) and with an iso- or hyperechoic appearance relative to the adjacent liver in the late phase. In these hemangiomas the progressive fill-in involves both the periphery and the center of the lesion at the same time during the arterial and late phases.

Hypervascular liver hemangiomas usually display rapid fill-in with diffuse contrast enhancement (Figs. 11.10, 11.11) during the arterial phase (Quaia et al. 2002a, 2004). Rapidly filling hemangiomas usually measure less than or equal to 3 cm, and correspond to roughly 16% of all hemangiomas

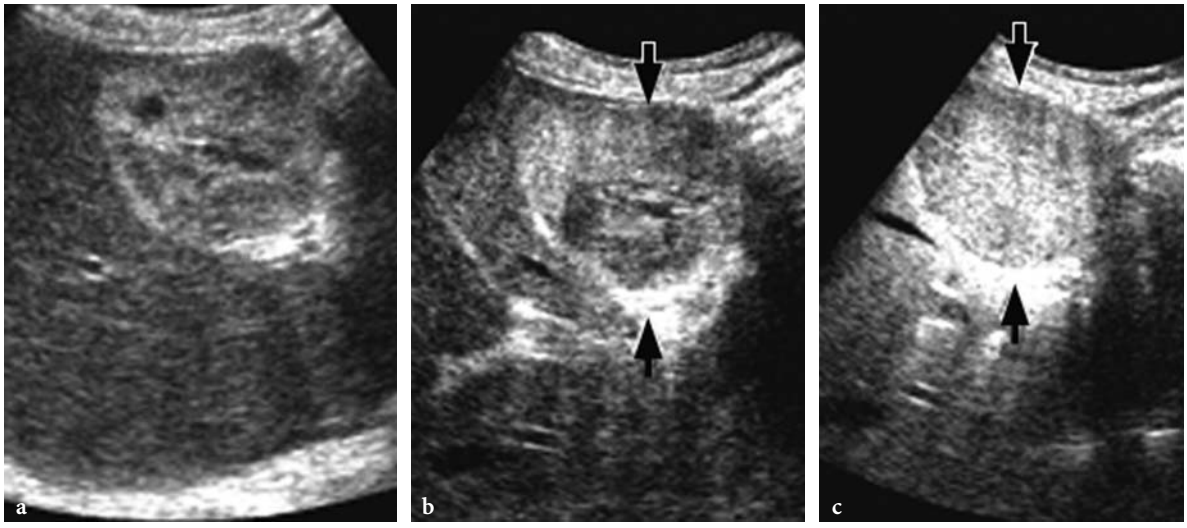

Fig. 11.9a–c. Hemangioma: progressive fill-in without nodular enhancement during the arterial phase. Longitudinal plane. **a** Baseline US. The hemangioma (*arrows*) appears hyperechoic and slightly heterogeneous. **b, c** Contrast-enhanced US. Contrast-specific mode: Pulse Inversion Mode (Philips-ATL, WA, USA) with high acoustic power insonation. Progressive centripetal fill-in without evidence of peripheral enhancement is demonstrated during the arterial (**b**) and late (**c**) phases.

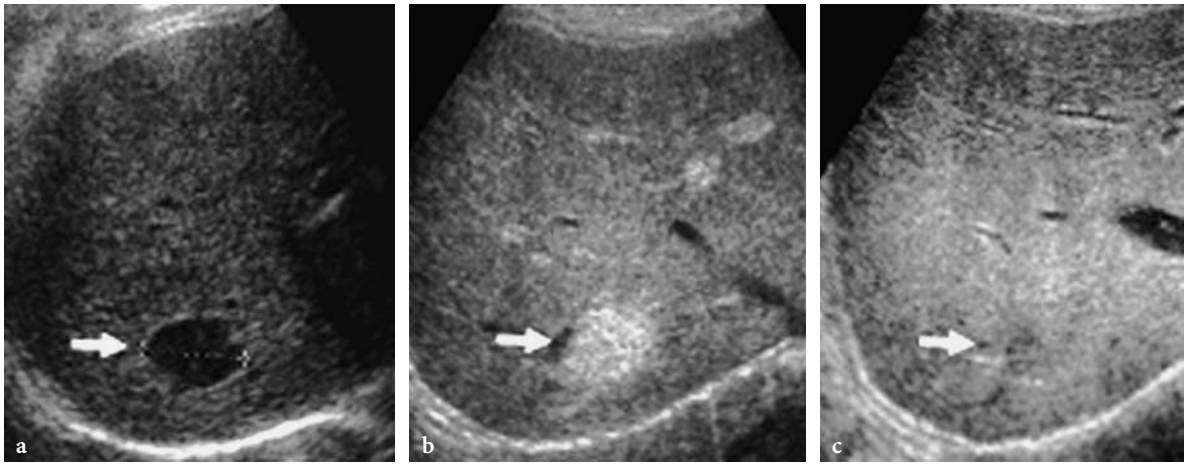

Fig. 11.10a–c. Hypervascular hemangioma: diffuse contrast enhancement. **a** Baseline US. A hypoechoic lesion (*arrow*) is demonstrated in a bright liver. **b, c** Contrast-enhanced US. Contrast-specific mode: Pulse Inversion Mode (Philips-ATL, WA, USA) with low acoustic power insonation. Diffuse homogeneous contrast enhancement demonstrated in the arterial phase (**b**) persists during the late phase (**c**), with a hyperechoic appearance in comparison to the adjacent liver parenchyma. Hemangioma was proved by US-guided biopsy.

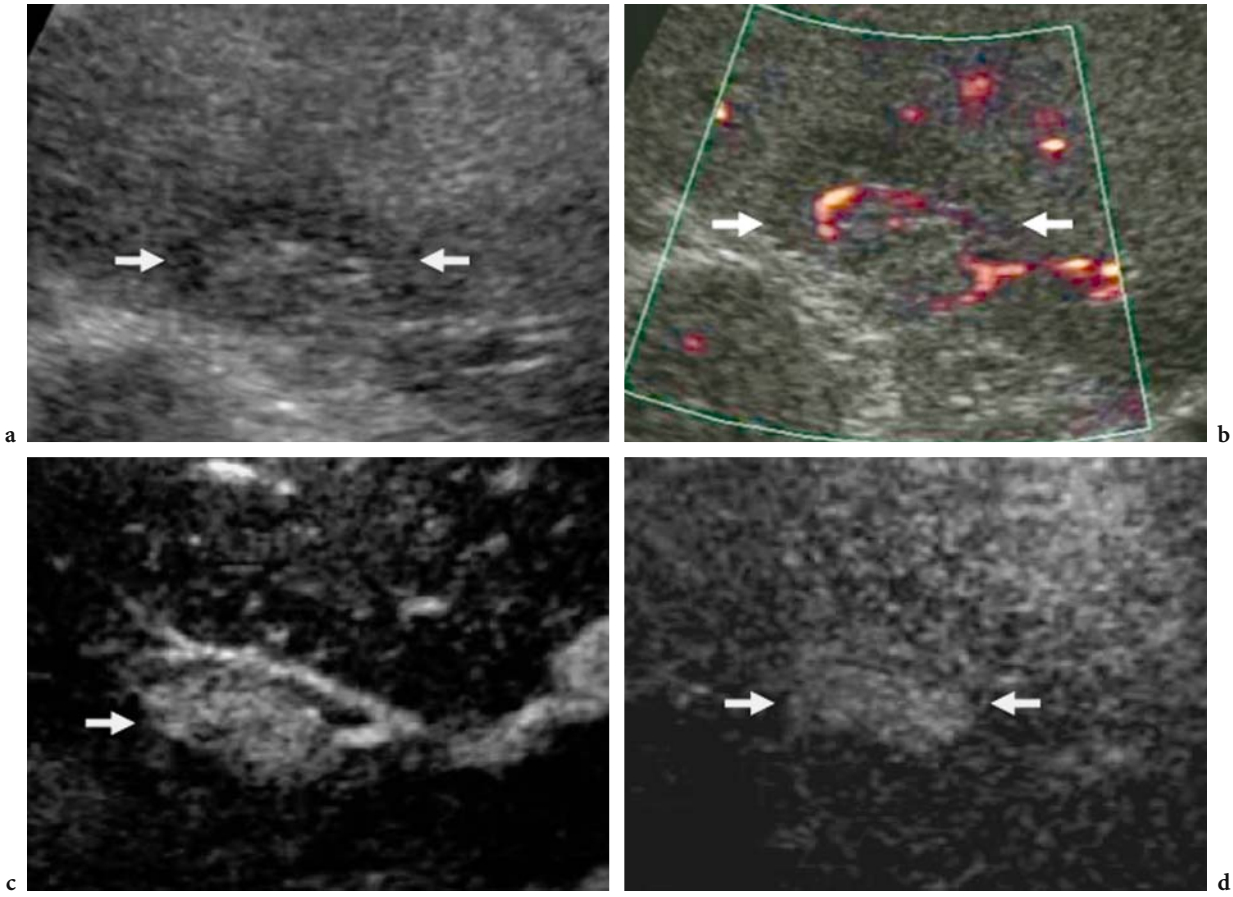

Fig. 11.11a–d. Hypervascular hemangioma: diffuse contrast enhancement. **a** Baseline US. A heterogeneous lesion (*arrows*) is demonstrated in a bright liver with some intratumoral vessels on baseline power Doppler US (**b**). **c, d** Contrast-enhanced US. Contrast-specific mode: Pulse Inversion Mode (Philips-ATL, WA, USA) with low acoustic power insonation. Diffuse homogeneous contrast enhancement is demonstrated during the arterial phase (**c**) and persists during the late phase (**d**), with an isoechoic appearance in comparison to the adjacent liver parenchyma. Hemangioma was proved by US-guided biopsy.

(Vilgrain et al. 2000); such hemangiomas are most commonly identified in cirrhotic patients (Brancatelli et al. 2001a). This enhancement pattern is similar to that observed on contrast-enhanced CT after the injection of iodinated contrast agents (Brancatelli et al. 2001a).

Persistent dotted contrast enhancement (Fig. 11.12) with an isovascular appearance relative to the adjacent liver may be observed in liver hemangiomas. This pattern is particularly frequent in liver hemangiomas with a hyperechoic appearance on baseline US (Quaia et al. 2002a) and is due to the difficulty in appreciating the vascularity and contrast enhancement in hyperechoic lesions (Koda et al. 2004). This pattern is quite frequent in hyperechoic liver hemangiomas after air-filled microbubble injection and intermittent high acoustic power insonation (Quaia et al. 2002a). It is more rarely observed after perfluorocarbon- or sulfur hexafluoride-filled microbubble injection at low acoustic power insonation, since this mode allows more effective suppression of the echo intensity of stationary tissues, thereby increasing the sensitivity to microbubble signals.

After microbubble injection, liver hemangiomas may also present a persistent hypoechoic appearance due to absence of contrast enhancement (Fig. 11.13), with or without rim-like peripheral enhancement. This enhancement pattern is frequently observed in thrombosed, fibrosclerotic, or hyalinized atypical liver hemangiomas, as proven using contrast-enhanced CT (Brancatelli et al. 2001a). In atypical liver hemangiomas, peripheral nodular enhancement with centripetal fill-in is often observed (Fig. 11.14).

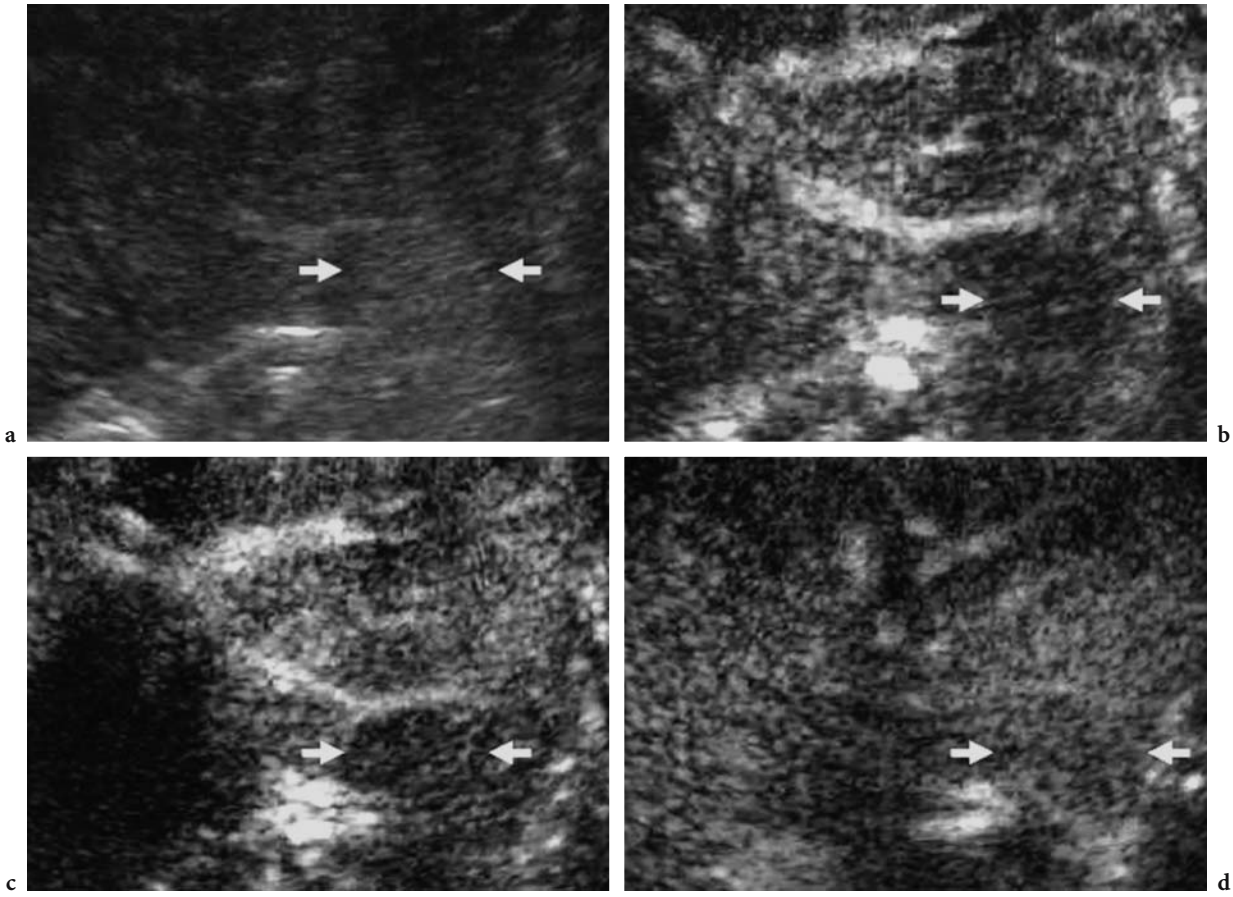

Fig. 11.12a–d. Hemangioma: dotted contrast enhancement. **a** Baseline US. A hyperechoic homogeneous lesion (*arrows*) is demonstrated. **b–d** Contrast-enhanced US. Contrast-specific mode: Contrast Tuned Imaging (Esaote, Genoa, Italy) with low acoustic power insonation. Dotted contrast enhancement is demonstrated in the arterial (**b**) and portal (**c**) phases, while there is an isoechoic appearance relative to the surrounding liver in the late phase (**d**).

11.3.2 Focal Nodular Hyperplasia

Epidemiology and histopathologic features. Focal nodular hyperplasia is the second most common benign tumor of the liver after liver hemangiomas, with an incidence of 1–3% (Karhunen 1986). Focal nodular hyperplasia is usually discovered as an asymptomatic incidental mass in young women who are undergoing imaging examinations for unrelated reasons and is multiple in 20% of cases. Focal nodular hyperplasia is up to eight times more common in women than in men, typically presents in the third to fifth decade, and measures less than 5 cm in size. The association of focal nodular hyperplasia with contraceptives is not definitely proven, even though pregnancy and oral contraceptive use can induce lesion growth. Focal nodular hyperplasia is probably caused by a hyperplastic response to a localized vascular abnormality (Wanless et al. 1985). Although focal nodular hyperplasia deserves conservative management, it may simulate the imaging characteristics of some malignant liver masses; therefore, correct preoperative diagnosis is essential. Focal nodular hyperplasia presents intratumoral hemorrhage or necrosis in up to 6% of cases (Sandler et al. 1980).

Histologically, focal nodular hyperplasia is composed of normal hepatic structures (hepatocytes, Kupffer cells, and bile ducts) which are abnormally arranged, and it is usually not capsulated. A distinct central scar and radiating fibrous septa are detected in the majority of cases (70–80%) upon analysis of the gross specimen. A fibromyxoid or fibrotic com-

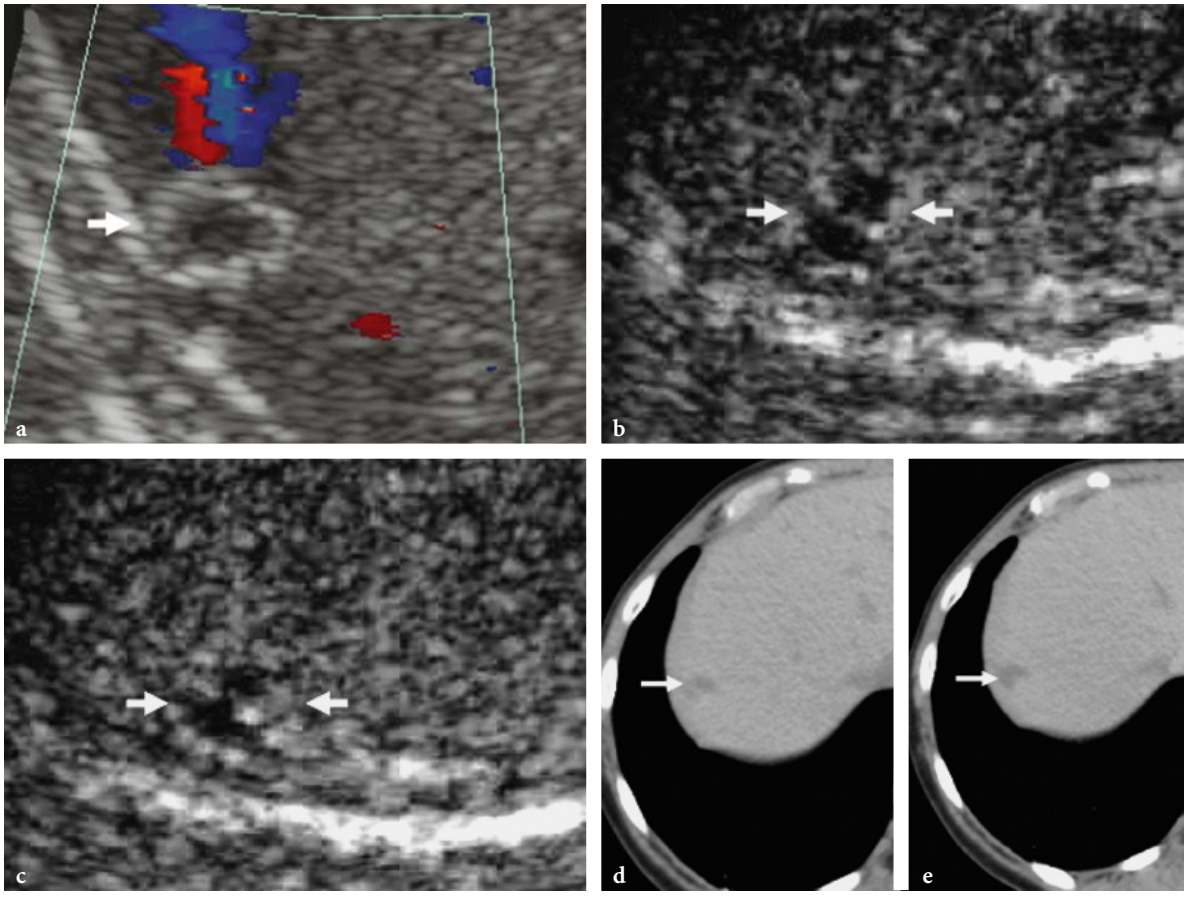

Fig. 11.13a–e. Hemangioma: absence of contrast enhancement in atypical liver hemangioma. **a** Baseline color Doppler US. A hypoechoic lesion with a peripheral hyperechoic rim and without evidence of peripheral or intralesional vessels is identified. **b, c** Contrast-enhanced US. Contrast-specific mode: Contrast Tuned Imaging (Esaote, Genoa, Italy) with low acoustic power insonation. There is no contrast enhancement during either the arterial (**b**) or the late (**c**) phase, and the lesion has a hypoechoic appearance relative to the surrounding liver. **d, e** Contrast-enhanced CT. Again, there is no evidence of contrast enhancement after iodinated contrast agent injection, the lesion having a hypodense appearance during both the arterial (**d**) and the late (**e**) phase. Hemangioma was proved by US-guided biopsy.

ponent may be present, depending on the degree of the liquid component, and there may be gross calcifications. In other cases, fibrous bands may be seen organizing the parenchymal architecture into lobules (Brancatelli et al. 2001b). Usually intratumoral calcifications, fat, and areas of necrosis are not identified.

Multimodality imaging – US and color Doppler US. Focal nodular hyperplasia usually appears homogeneously isoechoic or only slightly hyper- or hypoechoic compared to the adjacent liver. The characteristic spoke-wheel shaped pattern, with the central vessel radiating from the center to the periphery, can be identified at baseline color Doppler US. This pattern (Wang et al. 1997) is considered highly specific for focal nodular hyperplasia; however, its sensitivity is low since it is found in only 50% of cases, most frequently in larger lesions (Brancatelli et al. 2001b).

Multimodality imaging - CT. Focal nodular hyperplasia presents ill-defined smooth borders and a slightly hypodense or isodense appearance on nonenhanced CT, sometimes with evidence of the hypodense central scar. The lesion is frequently subcapsular and may present a mass effect with displacement of the adjacent blood vessels. Exophytic growth or distortion of the hepatic contour may be observed in about one-third of the lesions. After the injection of an iodinated contrast agent, the intratumoral feeding arteries, peripheral draining veins, and a peripheral pseudocapsule may be observed. During the arterial phase, focal nodular hyperplasia

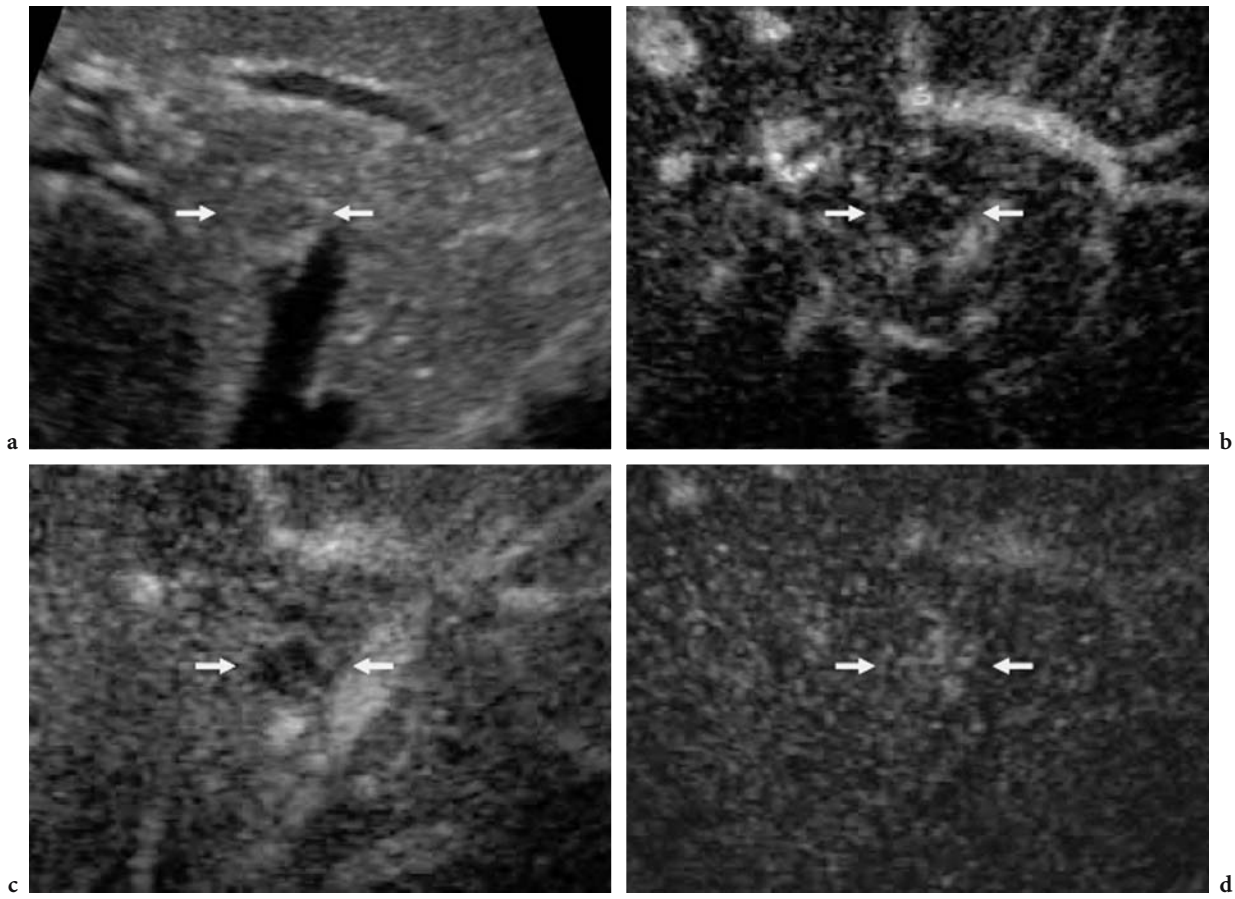

Fig. 11.14a–d. Hemangioma: peripheral nodular enhancement with centripetal fill-in in atypical liver hemangioma. **a** Baseline US. Atypical liver hemangioma with peripheral hyperechoic rim (*arrows*). **b–d** Contrast-enhanced US. Contrast-specific mode: Pulse Inversion Mode (Philips-ATL, WA, USA) with low acoustic power insonation. Peripheral nodular enhancement is demonstrated during the arterial phase (**b**), with progressive centripetal fill-in during the portal (**c**) and late (**d**) phases.

typically appears hyperattenuating relative to the adjacent liver, with a central hypoattenuating scar; the appearance is usually iso- or hyperattenuating during the portal and late phase scans. In the late phase, during the interstitial phase of iodinated contrast agent in the fibromyxoid tissue, the central scar more frequently appears hyper- or isoattenuating (Brancatelli et al. 2001b) in comparison with the rest of the lesion.

Multimodality imaging - MR. Focal nodular hyperplasia presents an isointense or slightly hyper- or hypointense appearance on nonenhanced T2-weighted sequences, while the central scar may appear hyper- or hypointense according to the liquid content of the fibromyxoid component. After the injection of a paramagnetic gadolinium-based contrast agent, the lesion appears hyperintense during the arterial phase due to diffuse contrast enhancement. A progressive reduction in contrast enhancement, leading to isointensity, is identified in the portal venous and late phases.

Administration of the liver-specific agent gadobenate dimeglumine (Gd-BOPTA) is essential to properly differentiate focal nodular hyperplasia from hepatocellular adenoma and malignant focal hepatic lesions (Grazioli et al. 2001b). Gd-BOPTA is a paramagnetic gadolinium-based contrast agent with a vascular–interstitial distribution in the initial minutes after injection and late biliary excretion of 2–4% of the administered dose after uptake by functioning hepatocytes (Kirchin et al. 1998; Spinazzi et al. 1999). At least 1 h after Gd-BOPTA administration, focal nodular hyperplasia appears generally

hyperintense (the central scar is hypointense) compared with adjacent liver, while other lesions appear isointense or slightly hypointense (Grazioli et al. 2001b). This hyperintensity is due to the prolonged and excessive hepatocellular accumulation of Gd-BOPTA in focal nodular hyperplasia, which lacks a well-formed bile canalicular system to allow normal excretion.

The administration of superparamagnetic iron oxide-based particulate agents, such as ferumoxides or ferucarbotran, which are taken up by the cells of the reticuloendothelial system, results in signal intensity loss on T2-weighted MR images (Bluemke et al. 2003; M.G. Kim et al. 2003) in focal nodular hyperplasia and other benign liver tumors containing reticuloendothelial cells. No such loss occurs in malignant liver tumors, with the exception of hepatocellular carcinomas with a reticuloendothelial intratumoral component.

Contrast-enhanced US. After the injection of air-filled microbubbles in the intermittent high acoustic power mode, focal nodular hyperplasia typically shows diffuse homogeneous contrast enhancement during the arterial phase. The intermittent insonation usually does not allow identification of the central spoke-wheel shaped contrast enhancement in the arterial phase. During the late phase, focal nodular hyperplasia typically shows persistent microbubble uptake similar to the adjacent liver (Blomley et al. 2001). This is due to the liver-specific properties of some air-filled microbubbles such as Levovist or Sonavist, which probably pool in sinusoids or are phagocytosed by Kupffer cells, in a manner similar to that observed when using sulfur colloid for scintigraphy or liver-specific contrast agents for MR imaging (Bluemke et al. 2003; M.G. Kim et al. 2003). During the late phase, the central scar, being devoid of sinusoids and Kupffer cells, is often evident since it is spared by microbubble uptake (Fig. 11.15).

After the administration of new generation sulfur hexafluoride- or perfluorocarbon-filled microbubbles for low acoustic power imaging, focal nodular hyperplasia may display central spoke-wheel shaped contrast enhancement (Fig. 11.16) during the first 10–15 s post injection (Albrecht et al. 2003; Nicolau et al. 2003a; Quaia et al. 2003, 2004), often with evidence of peripheral tortuous draining vessels. During the following seconds there is persistent diffuse homogeneous contrast enhancement, with a hyper- or isoechoic appearance relative to the adjacent liver during the late phase (Quaia et al. 2004). In cases of focal nodular hyperplasia smaller than 3 cm, the central spoke-wheel shaped contrast enhancement is more rarely observed, and diffuse contrast enhancement is immediately seen during the whole arterial phase. In the late phase the central scar may appear evident as a central hypoechoic region (Fig. 11.17) spared by microbubbles (Albrecht et al. 2003; Nicolau et al. 2003a; Quaia et al. 2003, 2004). This is because microbubble-based agents are purely intravascular agents and do not present any leakage into the interstitium during the late phase, a process that causes scar enhancement on contrast-enhanced CT and MR imaging.

11.3.3 Hepatocellular Adenoma

Epidemiology and histopathologic features. Hepatocellular adenoma is a rare benign hepatic neoplasm. Risk factors are use of estrogen- or androgen-containing steroid medications (the risk being related to the dose and duration) and the presence of type I glycogen storage disease (Grazioli et al. 2001a). The clinical presentation is usually pain due to mass effect (40%) or intratumoral or intraperitoneal hemorrhage (40%); it is an asymptomatic incidental finding in the remaining 20% of cases. Hepatocellular adenomas usually measure 8–10 cm at presentation, may be multiple (more than 10), are frequently encapsulated, and may be difficult to differentiate from other benign or malignant hepatic tumors (Ichikawa et al. 2000). Adenomas present intratumoral hemorrhage or necrosis in up to 60% of cases (Sandler et al. 1980).

Adenoma cells are larger than normal hepatocytes and contain large amounts of glycogen and lipid, which gives the characteristic yellow appearance of the cut surface. The propensity to hemorrhage reflects the histologic characteristics of adenomas, which consist of large plates of cells separated by dilated sinusoids that are perfused by arterial pressure since adenomas lack a portal venous supply and are fed solely by peripheral arterial feeding vessels. The extensive sinusoids and feeding arteries account for the hypervascular nature of hepatocellular adenoma, and the poor connective tissue support also predisposes to hemorrhage. Bile ductules are notably absent, as are Kupffer cells, a key histologic feature that helps distinguish hepatocellular adenoma from focal nodular hyperplasia. Malignant trans-

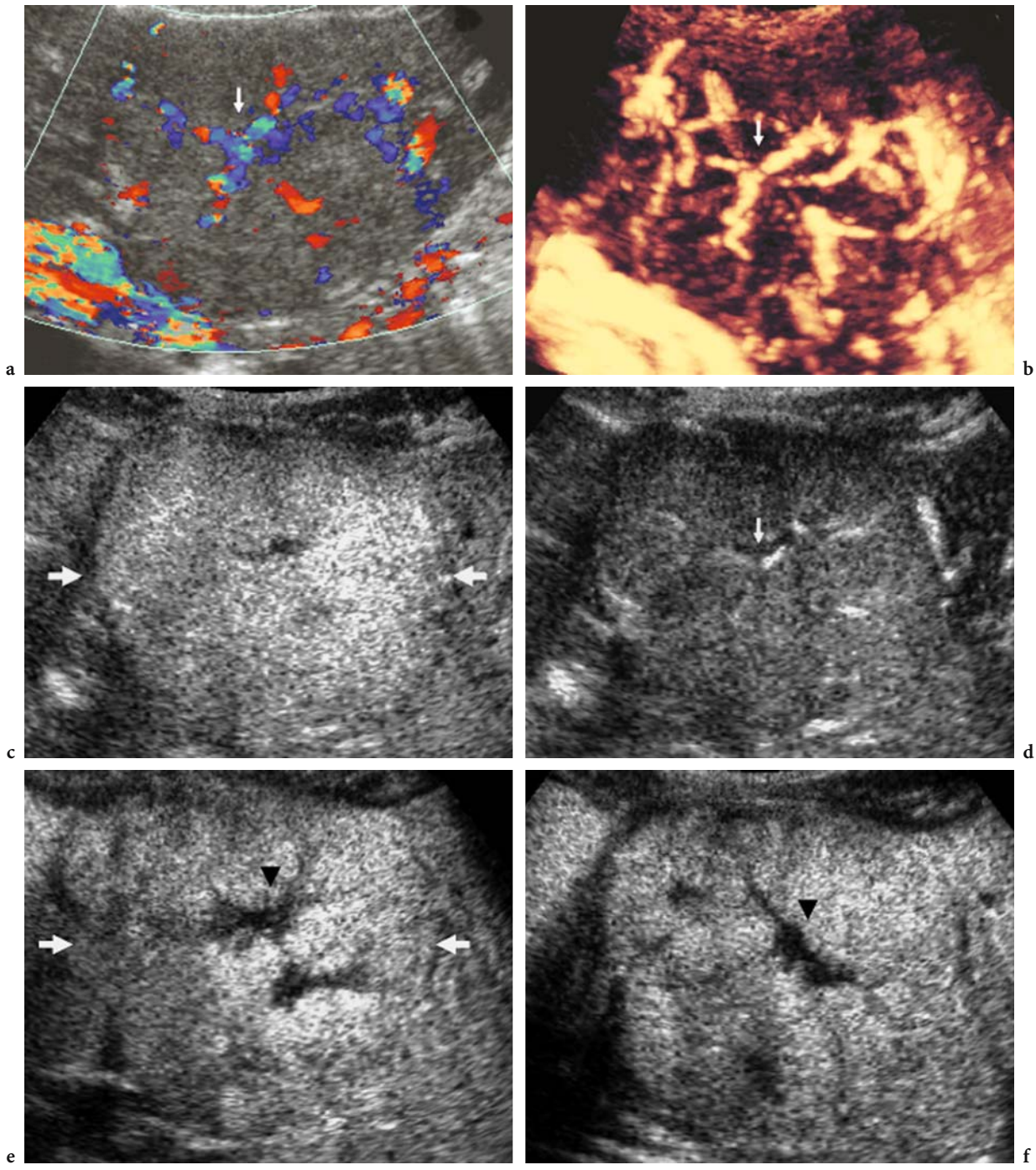

Fig. 11.15a–f. Focal nodular hyperplasia: spoke-wheel shaped contrast enhancement. **a, b** Baseline color (**a**) and power (**b**) Doppler. The central spoke-wheel shaped pattern (*arrow*) is identified, with a central vessel branching toward the periphery. **c–f** Contrast-enhanced US. Contrast-specific mode: Pulse Inversion Mode (Philips-ATL, WA, USA) after air-filled microbubble injection with high acoustic power insonation and production of four frames after each insonation. Diffuse homogeneous (*arrows*) contrast enhancement is evident during the arterial phase in the first frame of the train (**c**), while intratumoral vessels with a spoke-wheel shaped appearance (*arrow*) are identified in the second frame of the train (**d**). Diffuse contrast enhancement (*arrows*) persists in the late phase (**e, f**), sparing a central hypoechoic region (*black arrowhead*) that corresponds to the central scar.

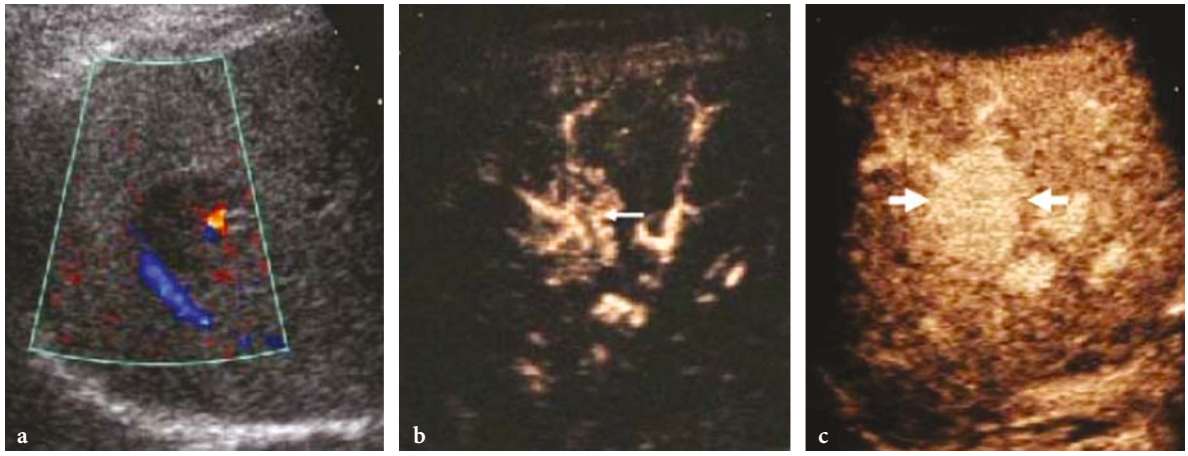

Fig. 11.16a–c. Focal nodular hyperplasia: central spoke-wheel shaped contrast enhancement pattern. Axial plane. **a** Baseline color Doppler US. Central vessels are identified in a hypoechoic focal liver lesion. **b, c** Contrast-enhanced US. Contrast-specific mode: Cadence Contrast Pulse Sequence (Siemens-Acuson, CA, USA). Central spoke-wheel shaped (*arrow*) contrast enhancement is evident 12 s after SonoVue injection (**b**). During the late phase (**c**), contrast enhancement remains diffuse, the lesion appearing isoechoic (*arrows*) relative to the surrounding liver.

Fig. 11.17a–c. Focal nodular hyperplasia: diffuse contrast enhancement pattern. Axial plane. **a** Baseline US. A slightly hyperechoic lesion (*arrows*) is identified. **b, c** Contrast-enhanced US. Contrast-specific mode: Coherent Contrast Imaging (Siemens-Acuson, CA, USA). Diffuse (*arrows*) contrast enhancement is evident 20 s after SonoVue injection (**b**), with evidence of some peritumoral tortuous draining vessels. In the late phase (**c**), contrast enhancement remains diffuse and the lesion has a hyperechoic appearance with evidence of a central hypoechoic region, corresponding to the central scar (*arrow*).

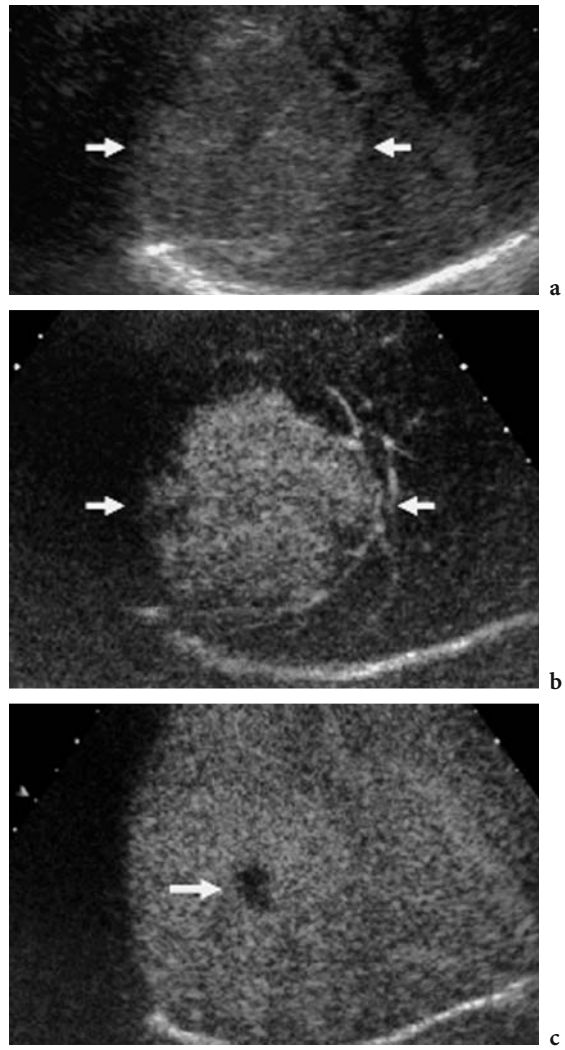

formation into hepatocellular carcinoma has been described (Brancatelli et al. 2002a).

Multimodality imaging – US and color Doppler US. The sonographic appearance of hepatocellular adenoma is variable and nonspecific. Most commonly it appears as a well-defined hyperechoic mass that is heterogeneous in terms of size and presence of hemorrhage and necrosis. The high lipid content of hepatocytes may result in variable to uniform hyperechogenicity within the lesion. No vascular pattern is considered specific for hepatocellular adenomas on color Doppler US (Golli et al. 1994), though subcapsular peripheral arteries and intranodular veins have been described (Bartolozzi et al. 1997).

Multimodality imaging - CT. Histotype diagnosis of hepatocellular adenoma is often difficult with CT even though it may reveal some typical features (Mathieu et al. 1986; Welch et al. 1985; Ichikawa et al. 2000). The areas of fat may be identified on nonenhanced CT as low-attenuation intratumoral

components, while areas of acute tumoral or subcapsular hemorrhage appear as heterogeneous hyperattenuating fluid. Necrosis and hemorrhage are identified in about one-fourth of hepatocellular adenomas (Ichikawa et al. 2000). Calcifications are rare and appear as large, coarse calcific opacities within areas of hemorrhage or necrosis.

The attenuation of the adenoma relative to the surrounding liver parenchyma varies depending on the composition of the tumor and that of the liver, as well as the phase of contrast enhancement after injection of iodinated contrast agent.

In patients with fatty liver, hepatocellular adenoma usually appears hyperattenuating during all phases of contrast enhancement. In normal liver, hepatocellular adenoma appears hyperattenuating during the arterial phase and isodense to the liver during the portal and late phases. It may have a homogeneous or heterogeneous appearance, the latter being particularly frequent when the lesion size exceeds 3 cm, and there is often evidence of a hyperattenuating tumoral capsule.

Multimodality imaging - MR. Hepatocellular adenoma shows diffuse contrast enhancement during the arterial phase after paramagnetic contrast agent injection, often with a heterogeneous appearance due to the intratumoral hemorrhagic or necrotic component. A hypointense appearance compared to adjacent liver 1 h after administration of Gd-BOPTA is considered typical since this lesion is devoid of biliary structures (Grazioli et al. 2001a).

Contrast-enhanced US. After microbubble injection, hepatocellular adenoma displays diffuse homogeneous or heterogeneous contrast enhancement. It may show either a persistent iso- or slightly hyperechoic appearance relative to the adjacent liver up until the late phase or a heterogeneous appearance. Whether hepatocellular adenomas display a homogeneous (Fig. 11.18) or heterogeneous (Fig. 11.19) appearance during each dynamic phase depends on the extent of the hemorrhagic and necrotic intratumoral component. Pericapsular feeding blood vessels are best visualized in the early arterial phase, while in the portal and late phases hepatocellular adenoma usually presents the same vascular behavior as the surrounding liver parenchyma (Quaia et al. 2004).

11.3.4 Macroregenerative and Dysplastic Nodules

Epidemiology and histopathologic features. Liver cirrhosis is preceded by varying pathologic parenchymal changes, including steatosis, inflammation, and edema, before the irreversible stages of fibro-

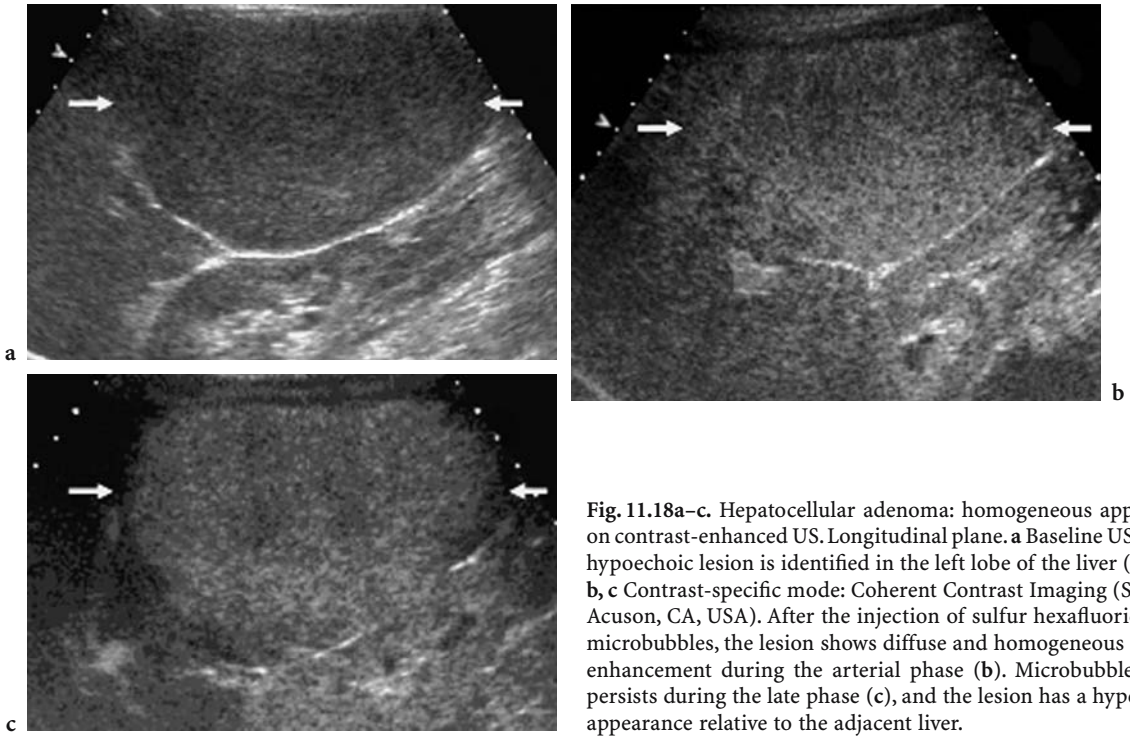

Fig. 11.18a–c. Hepatocellular adenoma: homogeneous appearance on contrast-enhanced US. Longitudinal plane. **a** Baseline US. A large hypoechoic lesion is identified in the left lobe of the liver (*arrows*). **b, c** Contrast-specific mode: Coherent Contrast Imaging (Siemens-Acuson, CA, USA). After the injection of sulfur hexafluoride-filled microbubbles, the lesion shows diffuse and homogeneous contrast enhancement during the arterial phase (**b**). Microbubble uptake persists during the late phase (**c**), and the lesion has a hyperechoic appearance relative to the adjacent liver.

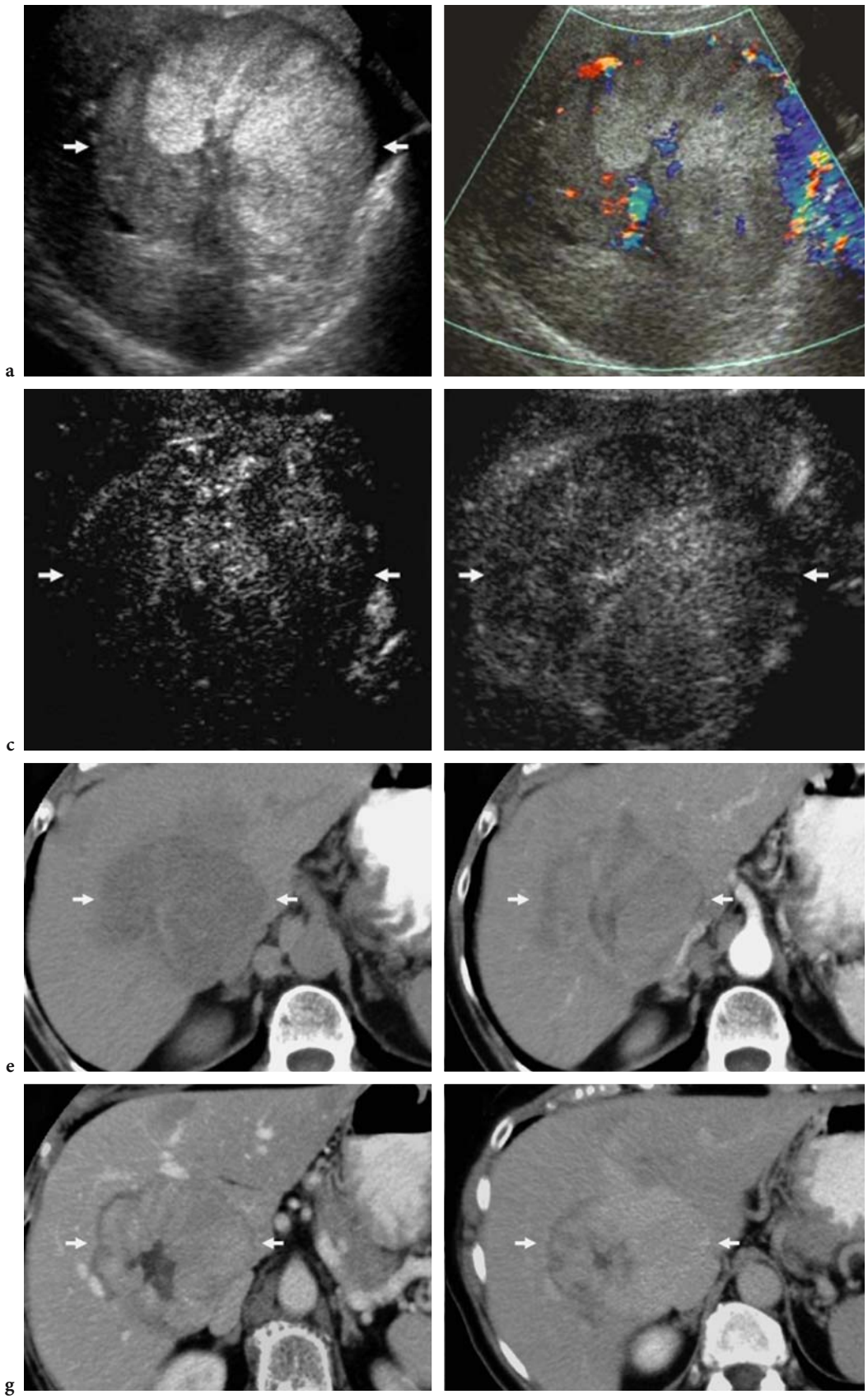
a
b
c
d
e
f
g
h

▷▷

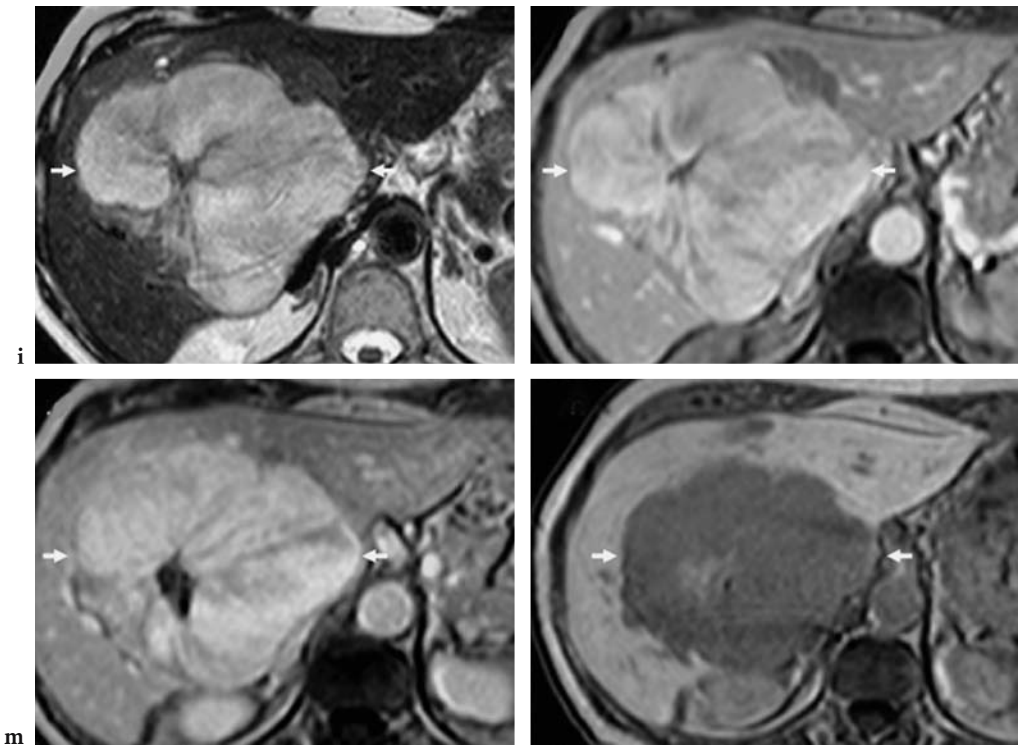

Fig. 11.19a–n. Hepatocellular adenoma: heterogeneous appearance on contrast-enhanced US. Axial plane. **a, b** Baseline US and color Doppler US. The lesion (*arrows*) has a heterogeneous appearance on baseline US (**a**) and peripheral and intratumoral vessels are demonstrated on color Doppler US (**b**). **c, d** Contrast-specific mode: Pulse Inversion Mode (Philips-ATL, WA, USA) after the injection of sulfur hexafluoride-filled microbubbles. Diffuse and heterogeneous contrast enhancement (*arrows*) appears 20 s after microbubble injection (**c**). The lesion (*arrows*) shows persistent microbubble uptake during the late phase (**d**), with a heterogeneous appearance. **e–h** Nonenhanced (**e**) and iodinated contrast-enhanced (**f–h**) CT scan. The hepatocellular adenoma (*arrows*) appears heterogeneous on the nonenhanced scan (**e**) and presents persistent and heterogeneous contrast enhancement during the arterial (**f**), portal (**g**), and late (**h**) phases. **i–n** Nonenhanced (**i**) and Gd-BOPTA-enhanced (**l–n**) MR scan. The hepatocellular adenoma (*arrows*) appears hyperintense on T2-weighted turbo spin echo nonenhanced scan (**i**) and presents diffuse and heterogeneous contrast enhancement during the arterial (**l**) and portal (**m**) phases. A diagnostic hypointense appearance is seen at 1 h post injection on the delayed scan (**n**).

sis and nodular regeneration occur (Baron and Peterson 2001).

Nodular lesions within the liver parenchyma can be separated into three broad categories: regenerative, dysplastic, or neoplastic. Regenerative nodules represent a region of parenchyma enlarged in response to necrosis, altered circulation, or other stimuli and may be observed both in noncirrhotic liver pathologies and in cirrhosis. The correct term for nodules larger than 5 mm in diameter is macroregenerative nodules or large regenerative nodules. Nodules smaller than 5 mm are usually not identified by imaging, even though they may give rise to a heterogeneous appearance of liver parenchyma.

In the absence of surrounding fibrous stroma, such nodules are also known as nodular regenerative hyperplasia (Baron and Peterson 2001). Nodular regenerative hyperplasia is frequently observed in many hepatic vascular disorders or systemic conditions such as Budd-Chiari syndrome (Brancatelli et al. 2002a), autoimmune disease, myeloproliferative disorders, and lymphoproliferative disorders.

When the macroregenerative nodule is surrounded by fibrous septa and constitutes the entire region banded by septa, it is also called a regenerative nodule on the basis of surrounding parenchymal attributes. When larger than 2 cm, macroregenerative nodules are usually dysplastic and contain cellular atypia without frank malignant changes (Baron and Peterson 2001).

Dysplastic nodules in the liver are nodular hepatocellular proliferations lacking the definite histopathologic criteria for malignancy (Kim et al. 2002). They contain cellular atypia without frank malignant changes and are sometimes precursors to frank hepatocellular carcinoma. Low-grade (adenomatous

hyperplasia) and high-grade (atypical adenomatous hyperplasia) dysplastic nodules may be identified, and a prevalently portal blood flow in macroregenerative nodules and arterial blood flow in dysplastic nodules has been reported (Kim et al. 2002). Although low-grade dysplastic nodules have a somewhat higher prevalence of portal blood supply than high-grade dysplastic nodules, the portal and arterial supplies are very variable (Lim et al. 2000; Kim et al. 2002).

Multimodality imaging. Macroregenerative nodules usually show a hypoechoic appearance on baseline US, and often they appear heterogeneous. On color Doppler US, macroregenerative nodules display peripheral arterial and venous vessels (Quaia et al. 2002c).

Findings on CT during arterial portography and CT during hepatic arteriography correlated positively with histologic grading. An overlap in appearance with dysplastic nodules and hepatocellular carcinomas was observed (Hayashi et al. 1999, 2002).

Macroregenerative nodules may appear hyperdense on nonenhanced CT. After the injection of iodinated contrast agent they usually display a hypodense appearance during the arterial phase, and progressively appear isodense relative to adjacent liver parenchyma during the late phase (Baron and Peterson 2001). Typically, macroregenerative nodules show low signal intensity on T2-weighted MR images, variable signal intensity on T1-weighted images, and no enhancement on arterial phase dynamic gadolinium-enhanced images (Hussain et al. 2002).

Dysplastic nodules appear hyperdense on nonenhanced CT and become isoattenuating during the portal phase on contrast-enhanced CT (Baron and Peterson 2001). Dysplastic nodules may display diffuse contrast enhancement and may simulate hepatocellular carcinoma. MR imaging of large dysplastic nodules may show a distinct pattern of homogeneous high signal intensity on T1-weighted images and very low signal intensity on T2-weighted images due to the high iron content (Baron and Peterson 2001).

Contrast-enhanced US. After microbubble injection, most macroregenerative nodules show absent or persistent dotted contrast enhancement, with a

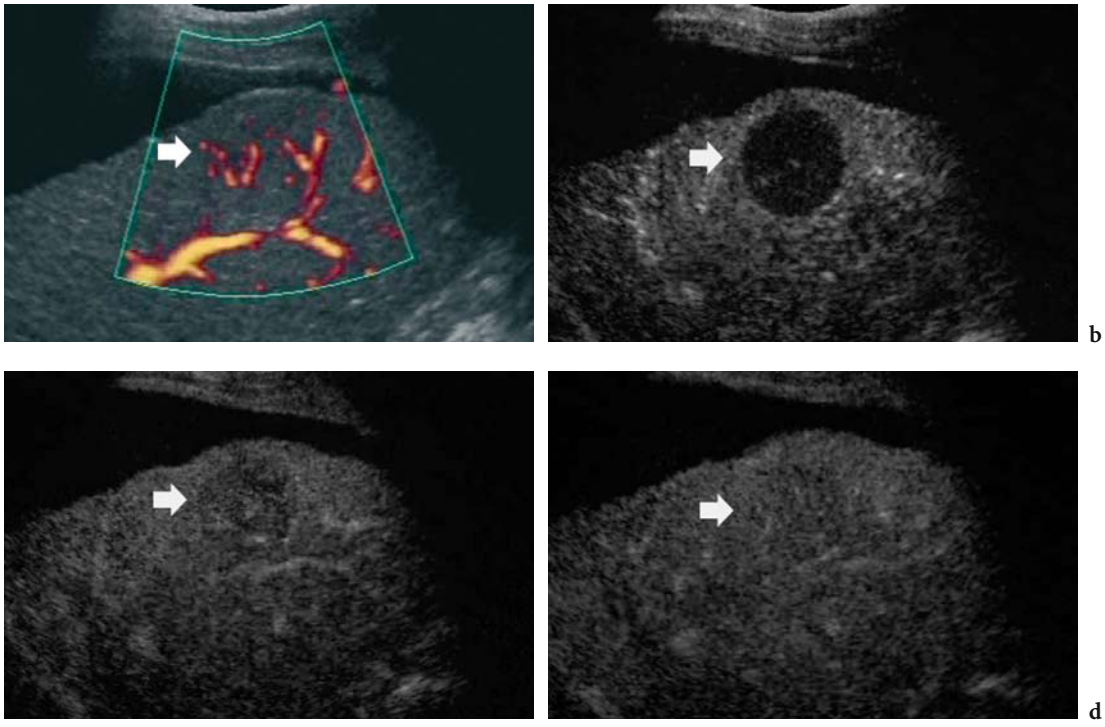

Fig. 11.20a-d. Macroregenerative nodule. **a** Baseline power Doppler US. An isoechoic lesion (*arrow*) with some intratumoral vessels is identified. **b–d** Contrast-enhanced US. Pulse Inversion Mode (Philips-ATL, WA, USA) with low acoustic power after injection of sulfur hexafluoride-filled microbubbles. There is absence of contrast enhancement in the arterial phase, the lesion having a hypovascular appearance (**b**). Progressively the lesion appears isoechoic relative to the adjacent liver during the portal (**c**) and late phases (**d**).

hypovascular or isovascular appearance during the arterial phase followed by an isovascular appearance during the late phase (Fig. 11.20) (Quaia et al. 2002b, 2004).

Dysplastic macroregenerative nodules may display diffuse (Quaia et al. 2004) contrast enhancement during the arterial phase. In relation to the adjacent liver, they appear iso- or hyperechoic in the arterial phase and isoechoic in the late phase (Fig. 11.21). A predominantly arterial blood flow is frequently present, this being the cause of the diffuse contrast enhancement (Kim et al. 2002). When diffuse contrast enhancement pattern is observed, consideration must be given to differentiation between dysplastic macroregenerative nodules and well-differentiated hepatocellular carcinomas, which may be difficult or even impossible, including at histologic assessment (Longchampt et al. 2000). Absence of contrast enhancement (Wen 2004) is related to a prevalently portal blood supply and arterial hypovascularity, as has been shown by other studies (Matsui et al. 1991). Development of hepatocellular carcinoma within high-grade dysplastic nodules of the liver may be identified by contrast-enhanced US (Nomura et al. 1993), on the basis of focal nodular intratumoral enhancement in the tumoral zone with malignant transformation ("nodule in nodule" pattern).

11.3.5 Focal Fatty Sparing and Focal Fatty Changes

Epidemiology and histopathologic features. Fatty infiltration of the liver is a well-characterized entity caused by accumulation of triglycerides within hepatocytes (Alpers and Isselbachers 1975). Fatty changes can be diffuse, even though heterogeneous distribution of fat is also frequently found. Nondiffuse fatty change of the liver, involving focal fatty deposition (Baker et al. 1985; Brawer et al. 1980; Halvorsen et al. 1982) and focal spared areas (Hirohashi et al. 2000; Kissin et al. 1986), appear as skip focal areas.

Multimodality imaging. On baseline US, focal fatty infiltration and focal fatty sparing are most commonly found adjacent to the gallbladder wall, the hepatic hilum, or the falciform ligament. Both focal

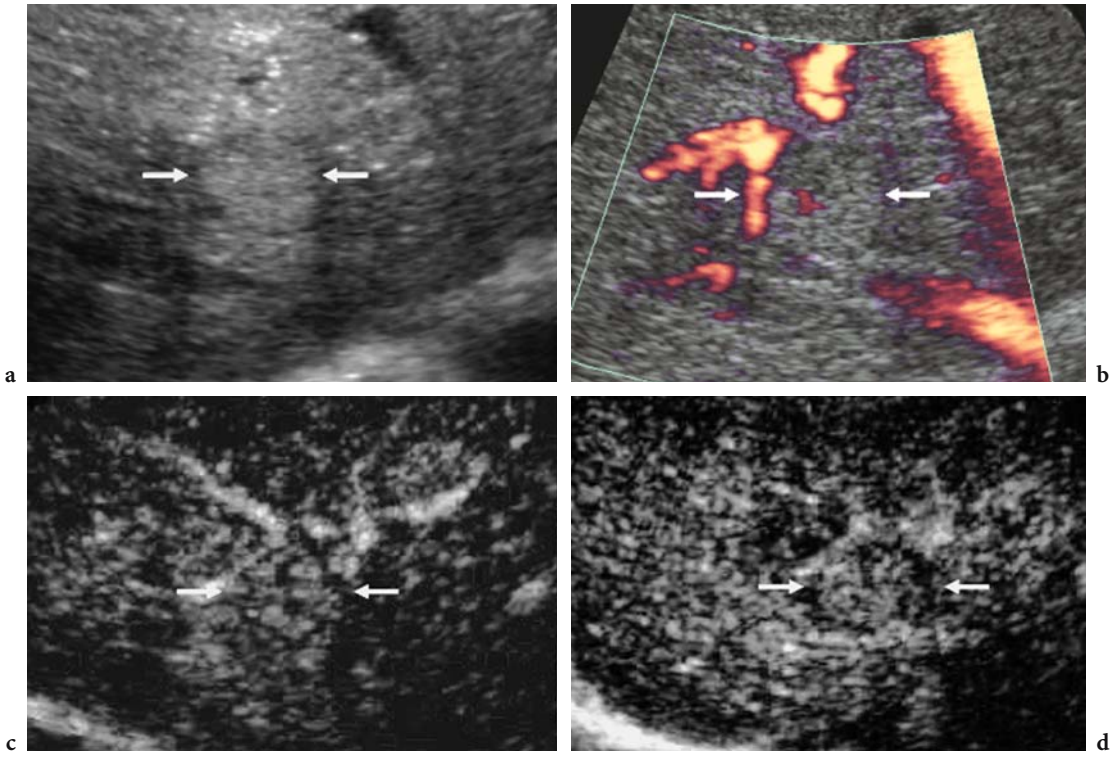

Fig. 11.21a–d. Dysplastic macroregenerative nodule. **a** Baseline US and **b** power Doppler US. Hyperechoic lesion (*arrows*) with one intratumoral vessel flow signal is identified. **c, d** Contrast-enhanced US. Contrast Tuned Imaging (Esaote, Genoa, Italy) with low acoustic power after the injection of sulfur hexafluoride-filled microbubbles. Diffuse contrast enhancement (*arrows*) is identified during the arterial phase (**c**), while the lesion has an isoechoic appearance relative to the adjacent liver in the late phase (**d**).

fatty infiltration and focal sparing may present a nodular or pseudonodular pattern which has to be differentiated from other focal liver lesions. Color Doppler US typically identifies normal vessels that run unaltered throughout the liver areas. On CT and MR imaging, both entities are easily differentiated from real tumors by the lack of a mass effect, undistorted vessels in the suspected area, and a similar grade of enhancement compared to the adjacent liver (Halvorsen et al. 1982; Kane et al. 1993).

Contrast-enhanced US. After microbubble injection, focal fatty sparing and focal fatty changes display homogeneous contrast enhancement with the same echo intensity as the adjacent normal liver parenchyma in the arterial, portal, and late phases (Fig. 11.22) (Nicolau et al. 2003a; Quaia et al. 2004).

11.3.6 Other Benign Focal Liver Lesions

Hepatic abscess. Hepatic abscesses are usually pyogenic (88%), amoebic (10%), or fungal (2%); 50% are multiple. On baseline US, colliquative liver abscess present an anechoic appearance with multiple heterogeneous spots at different levels. After microbubble injection, liver abscesses may present a similar appearance to hepatic malignancies since they show a hypoechoic appearance during the late phase (Albrecht et al. 2003) that may or may not be preceded by rim-like peripheral enhancement during the arterial phase (Fig. 11.23). The principal difference between liver abscesses and hepatic malignancies relates to the lesion shape and margins, which are coalescent and sharp in abscesses and round and ill-defined in malignancies (Kim et al. 2004a). Another important difference is the complete absence of vessels and enhancement in the central liquid portion of abscesses: even hypovascular metastases display some spots of weak contrast enhancement in the center of the lesion, except in the case of completely necrotic lesions (Albrecht et al. 2003).

Solitary necrotic hepatic nodule. This is a rare benign focal liver lesion which is often an incidental finding on US and may mimic a metastases (de Luca et al. 2000; Colagrande et al. 2003). Most reported cases of solitary necrotic nodule have been in males, and the majority of these lesions have occurred in the right hepatic lobe (Koea et al. 2003). At histologic analysis the solitary necrotic nodule is characterized by central coagulative necrosis, often partly calcified and surrounded by a dense hyalinized fibrous capsule containing elastin fibers (Koea et al. 2003). On US, the necrotic nodule usually appears hypoechoic or target-like with a hyperechoic center, while on contrast-enhanced CT and MR imaging no contrast enhancement is identified. After microbubble injection, the absence of contrast enhancement is evident (Fig. 11.24).

Other rare benign focal liver lesions may be identified and scanned after the injection of microbubble-based agents, e.g., inflammatory pseudotumor (chronic inflammatory cell infiltration and fibrosis), intrahepatic extramedullary hemato-

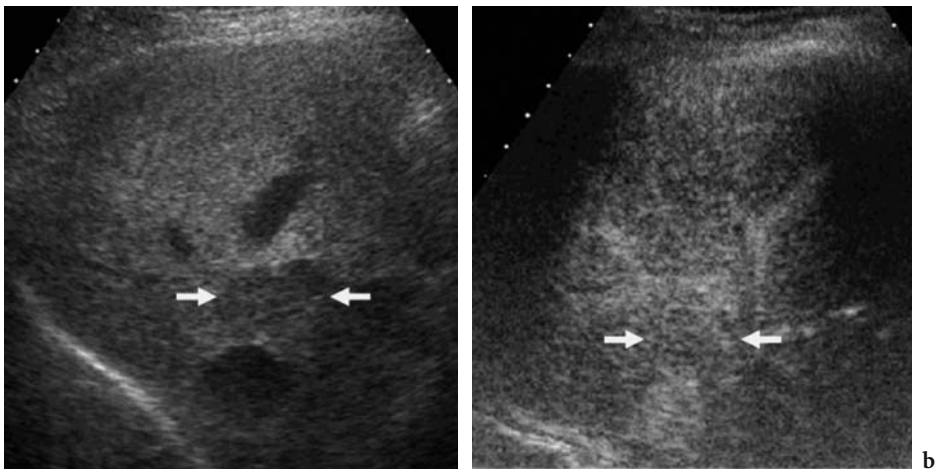

Fig. 11.22a,b. Region of focal fatty sparing. **a** Baseline US and **b** contrast-enhanced US during the late phase, 2 min after the injection of sulfur hexafluoride-filled microbubbles. The lesion (*arrows*) appears hypoechoic in a bright liver on baseline US but isoechoic during the late phase after microbubble injection.

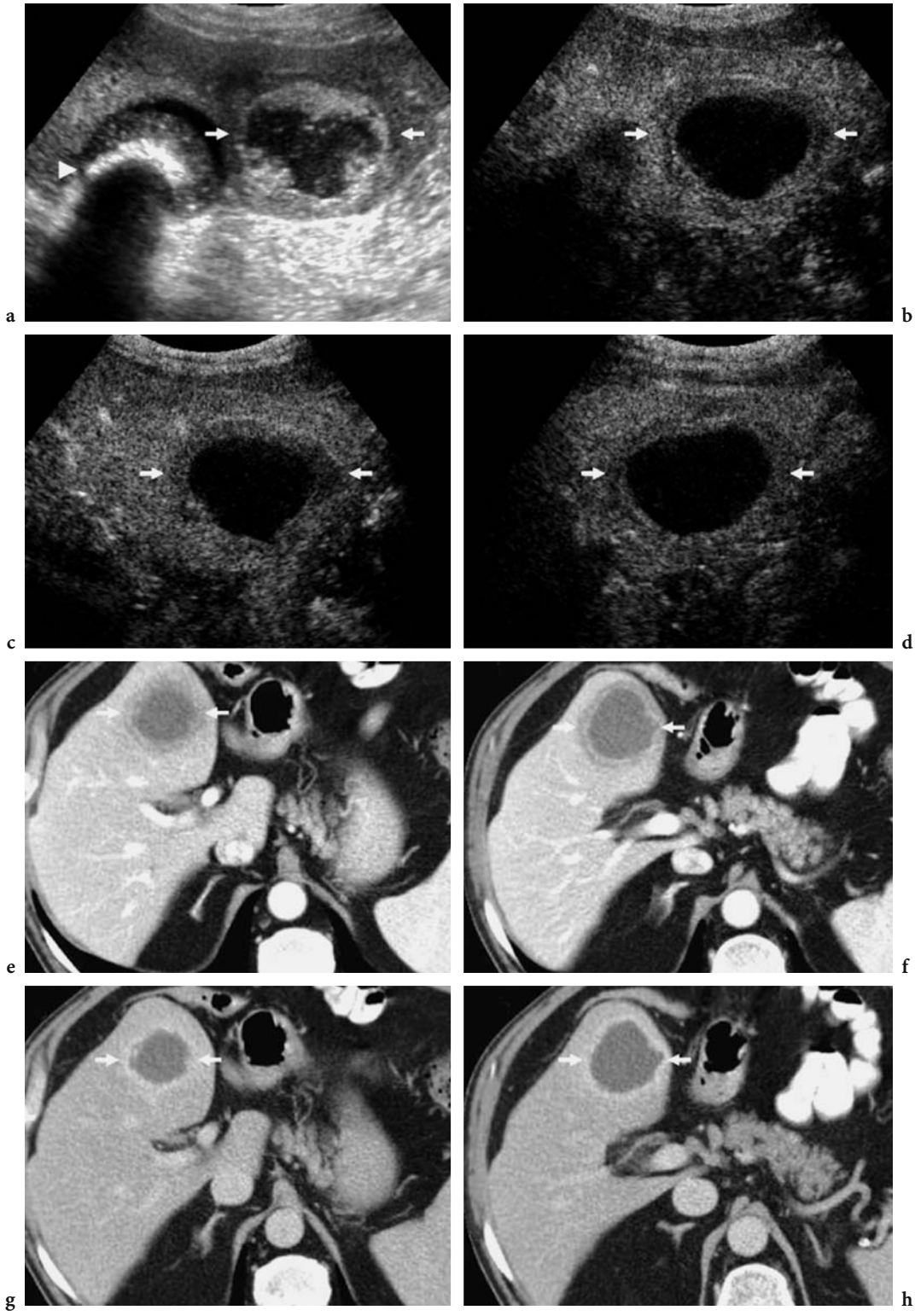

Fig. 11.23a–h. Liver abscess. **a** A heterogeneous lesion with a central hypoechoic component and a peripheral hyperechoic component adjacent to a calculous gallbladder is identified on baseline US. **b–d** After microbubble injection, the abscess demonstrates peripheral capsular enhancement sparing the central liquid portion. **e–h** On contrast-enhanced CT (iodinated contrast agent), the peripheral capsule displays progressively increasing contrast enhancement with a hyperdense appearance during the late phase, sparing the central liquid portion.

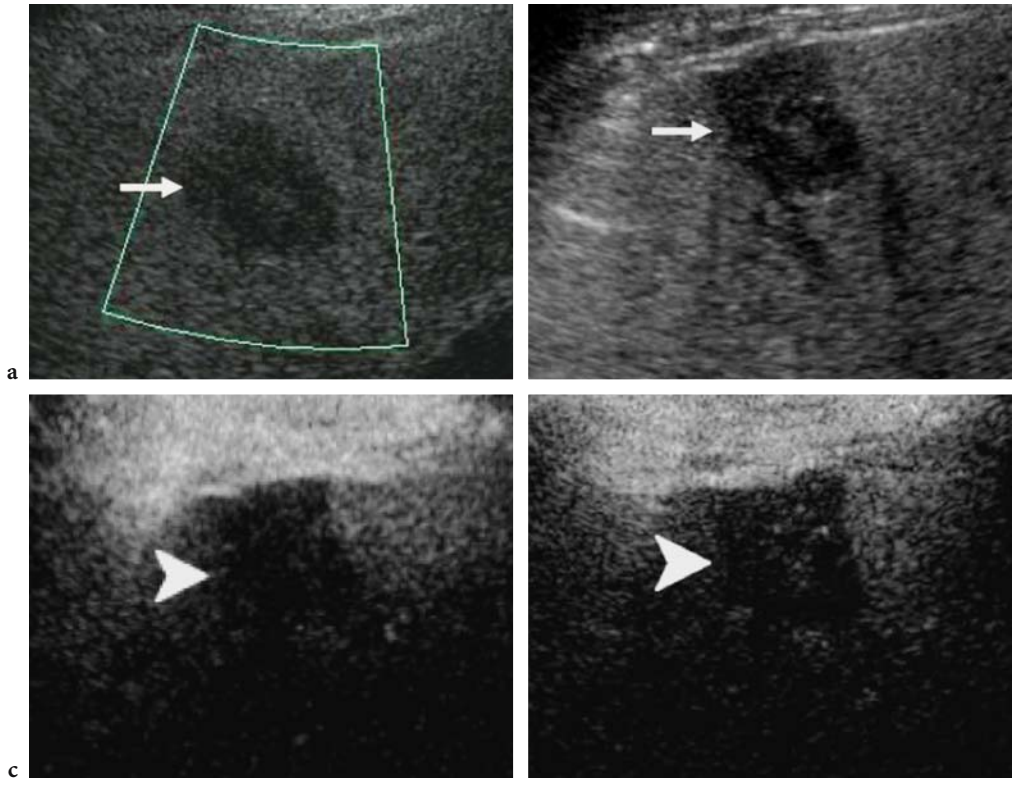

Fig. 11.24a–d. Solitary necrotic nodule. Axial plane. Contrast-enhanced US. Contrast-specific mode: Contrast Tuned Imaging (Esaote, Genoa, Italy) after the injection of sulfur hexafluoride-filled microbubbles. The lesion (*arrows*) appears hypoechoic on baseline US (**a**), with intratumoral vessels visible on color Doppler US (**b**). Contrast enhancement is absent in both the arterial (**c**) and the late phase (**d**). The lesion has a persistent hypoechoic appearance during the late phase (*arrowheads*).

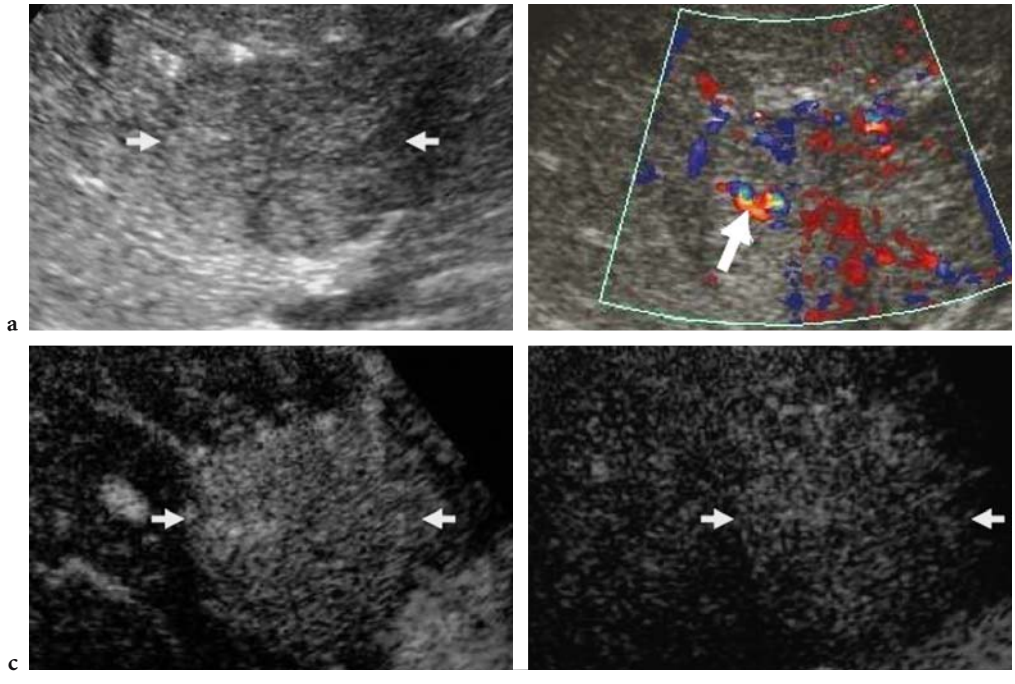

Fig. 11.25a–d. Intrahepatic extramedullary hematopoiesis. Axial plane. Contrast-enhanced US. Contrast-specific mode: Pulse Inversion Mode (Philips-ATL, WA, USA) after the injection of sulfur hexafluoride-filled microbubbles. The lesion (*arrows*) appears hypoechoic on baseline US (**a**), with intratumoral vessels (*arrow*) on color Doppler US (**b**). Diffuse contrast enhancement is identified during the arterial phase (**c**) and persists into the late phase (**d**), when the lesion continues to appear slightly hyperechoic relative to the surrounding liver.

poiesis (Fig. 11.25), and hepatic angiomyolipoma (Fig. 11.26). These lesions usually display a hypervascular pattern during the arterial phase, with persistent microbubble uptake in the late phase, as for the other benign focal liver lesions.

11.4 Malignant Focal Liver Lesions

11.4.1 Hepatocellular Carcinoma

Epidemiology and histopathologic features. Hepatocellular carcinoma is the most common primary liver malignancy and its incidence is increasing, particularly in Asia and Africa. The prevalence of hepatocellular carcinoma has been reported to be 14% among transplant recipients with cirrhosis in whom there was no suspicion of tumor before referral for transplantation (Peterson et al. 2000). Accordingly, it is strongly associated with cirrhosis (80% of patients) and also with chronic viral hepatitis, the greatest increase in risk being observed among patients with hepatitis B or C (Peterson et al. 2000; Baron and Peterson 2001). Hepatocellular carcinoma shows a propensity for venous invasion, with involvement of the portal vein (in 30–60% of cases) or hepatic vein (in 15%) and inferior vena cava. HCC may occur in three forms: solitary, multiple, and diffuse infiltrative (Larcos et al. 1998).

Multimodality imaging – US and color Doppler US. The appearance of hepatocellular carcinoma on baseline US is variable but there is a relationship with size. Hepatocellular carcinomas <3 cm (Ebara et al. 1986) predominantly appear hypoechoic, though small tumors may appear echogenic due to the presence of fatty changes or sinusoidal dilatation (Yoshikawa et al. 1988). A hypoechoic rim may be observed around small echogenic HCCs owing to the presence of a fibrous capsule; this assists in the differentiation from other focal liver lesions in the cirrhotic liver, such as hemangiomas. Large (>5 cm) hepatocellular carcinomas are predominantly hyperechoic and heterogeneous due to the presence of hemorrhage, fibrosis, and necrosis.

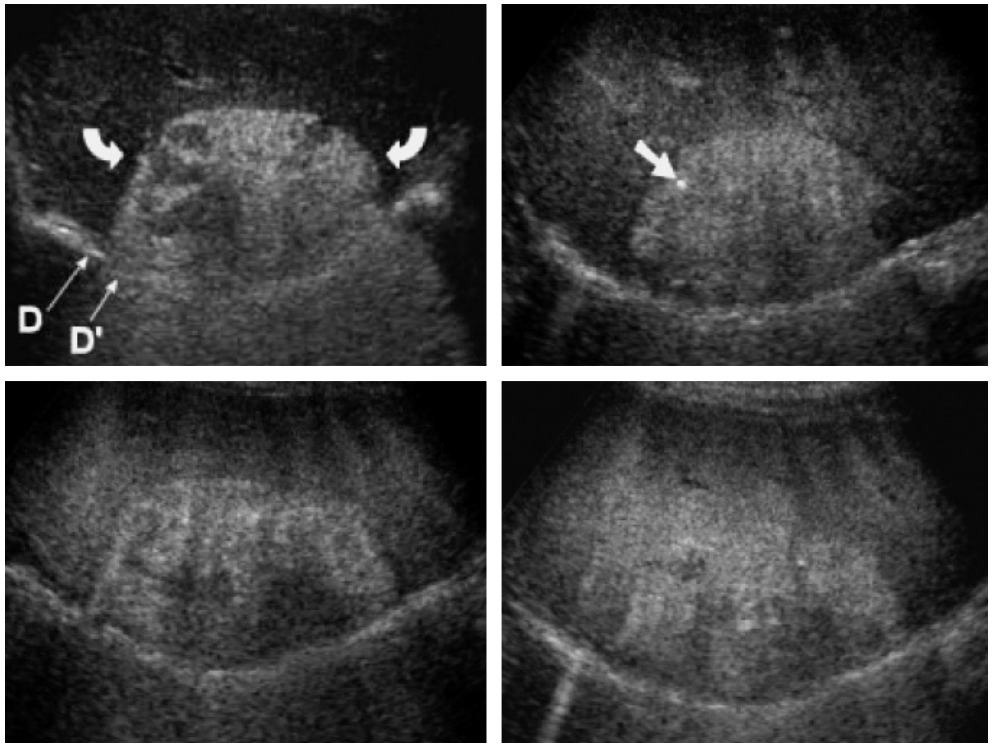

Fig. 11.26a–d. Hepatic angiomyolipoma. **a** Axial scan at baseline US shows a large, sharply marginated, heterogeneous and predominantly hyperechoic mass (*curved arrows*) with diffuse posterior acoustic enhancement. The segment of the diaphragm (*D'*) posterior to the hepatic mass appears displaced away from the rest of the diaphragm (*D*). This is due to an artifact caused by the lower US velocity in the fat of the angiomyolipoma compared with the adjacent liver parenchyma. **b–d** Contrast-enhanced US, 25 s (**b**), 60 s (**c**), and 120 s (**d**) after the injection of air-filled microbubbles. Heterogeneous contrast enhancement is identified, with evidence of intralesional vessels (*arrow* in **b**).

It has been demonstrated that color Doppler US can accurately assess the vascularity of hepatocellular carcinomas (Lencioni et al. 1996) for the purposes of differential diagnosis, choice of treatment, and assessment of therapeutic response. Color Doppler US with Doppler examination of tumor vessels shows high systolic and diastolic signals due to arteriovenous shunts and low-resistance vasculature. The basket pattern (Tanaka et al. 1992), consisting in peripheral arterial vessels branching toward the center of the lesion, is observed in about 75% of cases.

Multimodality imaging – CT and MR. Most hepatocellular carcinomas <3 cm are hypervascular and present diffuse contrast enhancement on CT and MR imaging, with contrast material washout in the portal venous phase (Nino-Murcia et al. 2000; Hussain et al. 2002). A minority of hepatocellular carcinomas <3 cm are hypovascular, with low or absent enhancement during the arterial phase (Hayashi et al. 2002); such cases are best identified on portal venous phase or equilibrium phase imaging as hypodense lesions. Large (>5 cm) hepatocellular carcinomas are heterogeneous, with characteristic findings such as the mosaic pattern (different well-demarcated tumoral zone with different density) (Stevens et al. 1996), a tumoral capsule, necrosis, and fatty metamorphosis (Hussain et al. 2002). A tumoral capsule is in fact present in 60–82% of large hepatocellular carcinomas (Hussain et al. 2002) and, typically, presents a hyperdense appearance during the late phase.

The signal intensity of hepatocellular carcinoma is variable on both T1-weighted and T2-weighted MR imaging sequences. Some hepatocellular carcinomas show a high signal intensity on T1-weighted images due to the presence of fat, copper, or glycoproteins (Baron and Peterson 2001; Hussain et al. 2002). After paramagnetic contrast agent injection, as on contrast-enhanced CT, enhancement is diffuse in smaller hepatocellular carcinomas and heterogeneous in larger cases. The evolution of a dysplastic nodule to hepatocellular carcinoma can be seen on MR imaging by virtue of the so-called nodule-in-a-nodule appearance (Mitchell et al. 1991; Hussain et al. 2002), with evidence of intratumoral contrast enhancement in the tumoral zone upon malignant transformation.

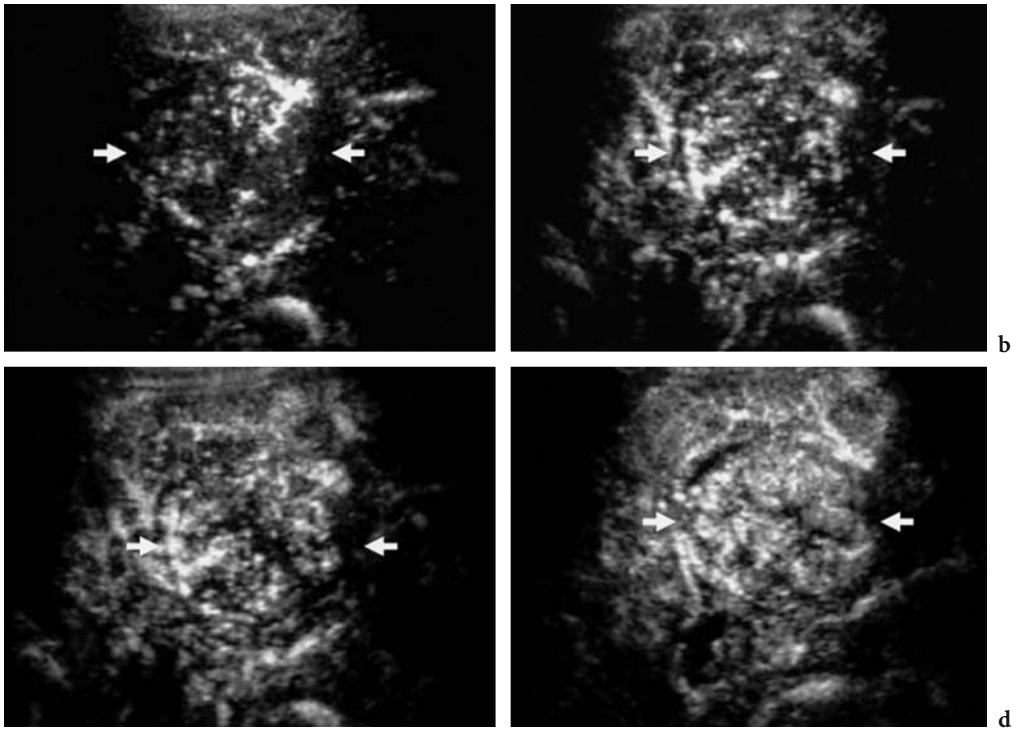

Fig. 11.27a–d. Hepatocellular carcinoma vascularity during the arterial phase after microbubble injection. Contrast-specific mode: Pulse Inversion Mode (ATL-Philips, WA, USA) with low acoustic power after the injection of sulfur hexafluoride-filled microbubbles. Within the hepatocellular carcinoma (*arrows*), peripheral and penetrating arterial vessels are observed during the first 15 (**a**) to 20 (**b**) s of the arterial phase. During the following seconds of the arterial phase (**c, d**), smaller intratumoral vessels also display contrast enhancement.

Contrast-enhanced US. After microbubble injection, intratumoral vessels are visualized in the majority of hepatocellular carcinomas during the arterial phase (Dill-Macky et al. 2002; Feruse et al. 2003; Isozaki et al. 2003; Wang et al. 2003; Cosgrove and Blomley 2004; Koda et al. 2004). The classic hemodynamics of hepatocellular carcinoma are characterized by evidence of tumor vessels and a hypervascular appearance during the arterial phase and by the absence of portal blood flow (Koda et al. 2004). Contrast-enhanced US has been shown to display tumor vessels during the first 15–20 s of the arterial phase (Fig. 11 27), with better accuracy than color Doppler US owing to the avoidance of motion and blooming artifacts (Koda et al. 2004).

Following the injection of microbubble-based agents, diffuse homogeneous or heterogeneous contrast enhancement (Figs. 11.28–11.31) is typically observed during the arterial phase (Choi et al. 2002; K.W. Kim et al. 2003), revealing the characteristic hypervascular nature of hepatocellular carcinoma. From 45 to 70 s after injection up to the late phase, hepatocellular carcinomas (whether smaller or larger than 3 cm) display a hypovascular (Figs. 11.28, 11.30) or isovascular (Figs. 11.29, 11.31) appearance compared to the adjacent liver, with or without evidence of peripheral hyperechoic rim-like enhancement.

The isovascular appearance of some hepatocellular carcinomas during the late phase is similar to that of benign focal liver lesions (Quaia et al. 2004). The reason for this atypical behavior is unclear. Possibly, the isoechoic appearance is caused by the recirculation of low levels of microbubbles, but further studies are necessary to determine whether histological or vascular differences exist in these cases. Some studies have correlated the appearance of hepatocellular carcinomas during the late phase with tumoral differentiation and identified better differentiation in hepatocellular carcinomas which appear isoechoic to the adjacent liver in the late phase (Nicolau et al. 2004).

Less frequently, hepatocellular carcinomas display persistent dotted contrast enhancement with either an initial hypovascular and late isovascular appearance (Quaia et al. 2004) or a persistent hypovascular appearance compared to the adjacent liver (Giorgio et al. 2004). This pattern resembles the hypovascular pattern described on CT (Hayashi et al. 2002) after the injection of iodinated agents.

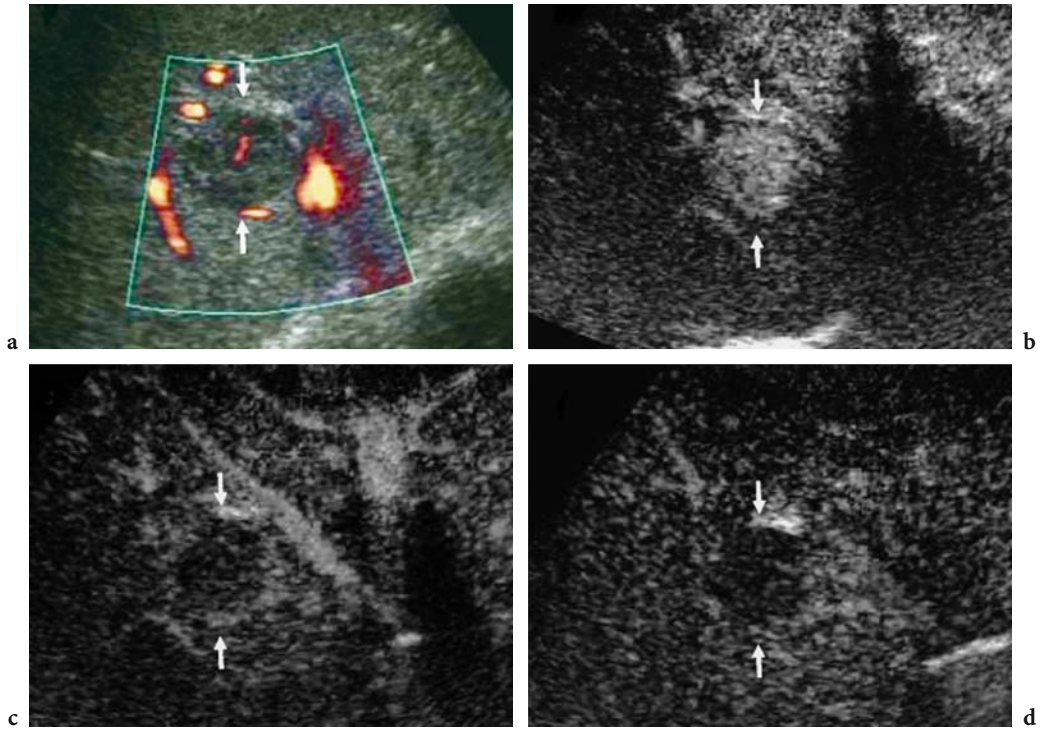

Fig. 11.28a–d. The most frequent and typical appearance of small hepatocellular carcinoma on contrast-enhanced US. Axial plane. **a** Baseline power Doppler US. The tumor (*arrows*) appears hypoechoic, with peripheral and intratumoral vessels. **b–d** Contrast-specific mode: Contrast Tuned Imaging (Esaote, Italy) with low acoustic power after the injection of sulfur hexafluoride-filled microbubbles. The hepatocellular carcinoma (*arrows*) presents diffuse homogeneous contrast enhancement with rapid microbubble washout and a hypovascular appearance during the portal (**c**) and late (**d**) phases, compared to the adjacent liver.

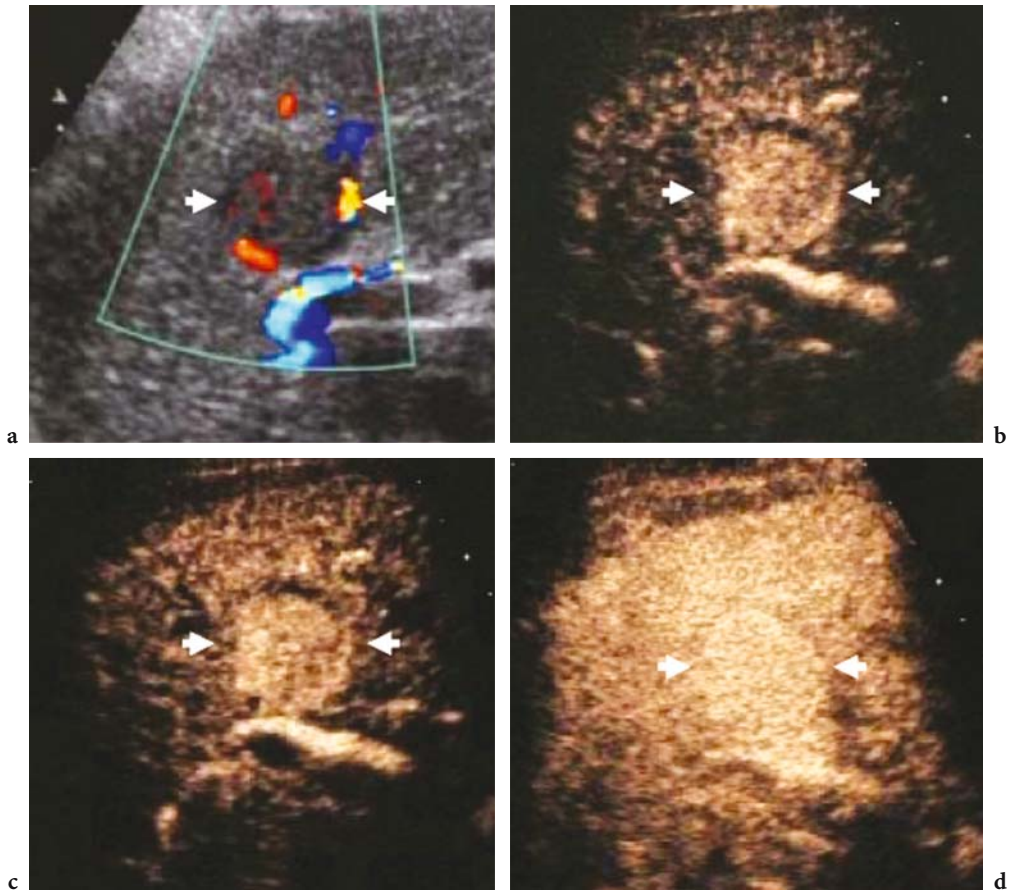

Fig. 11.29a–d. Small hepatocellular carcinoma with an isovascular appearance during the late phase on contrast-enhanced US. Longitudinal plane. **a** Baseline color doppler US. The tumour (*arrows*) presents prevalently peripheral vossels. **b–d** Contrast-specific mode: Cadence Contrast Pulse Sequence (Siemens-Acuson, CA, USA) with low acoustic power after the injection of sulfur hexafluoride-filled microbubbles. **b** Arterial phase (22 s after SonoVue injection). The hepatocellular carcinoma (*arrows*) presents diffuse and heterogeneous contrast enhancement. The tumor (*arrows*) appears isovascular to the adjacent liver during the portal phase (**c**=65 s after SonoVue injection) and the late phase (**d**=100 s after SonoVue injection).

Fibrolamellar hepatocellular carcinoma. The fibrolamellar type is a rare form (2%) of hepatocellular carcinoma occurring in younger females without coexisting liver disease and has a better prognosis than the common variety. It is typically large with a central stellate scar (Ichikawa et al. 1999; McLarney et al. 1999). Although it is important to distinguish fibrolamellar hepatocellular carcinoma from conventional hepatocellular carcinoma, it is equally important to distinguish it from certain benign liver lesions with a central scar, especially focal nodular hyperplasia, large hemangiomas (Blachar et al. 2002), and, rarely, hepatocellular adenomas. Calcifications are present in 40–68% of tumors, and areas of hypervascularity are heterogeneous in all cases. After the injection of iodinated or paramagnetic contrast agents for CT and MR imaging, respectively, a heterogeneous appearance was described during the arterial and portal phases, with evidence of a central scar, while a progressively homogeneous appearance was observed in the late phase (Ichikawa et al. 1999; McLarney et al. 1999). Fibrolamellar type hepatocellular carcinoma has been reported to present persistent rim-like or heterogeneous contrast enhancement with a hypoechoic appearance during the late phase (Quaia et al. 2004).

11.4.2 Metastases

Epidemiology and histopathologic features. Metastases are the more common malignant lesions of the liver in Europe and United States, in particular from tumors of the gastrointestinal tract (Ferrucci

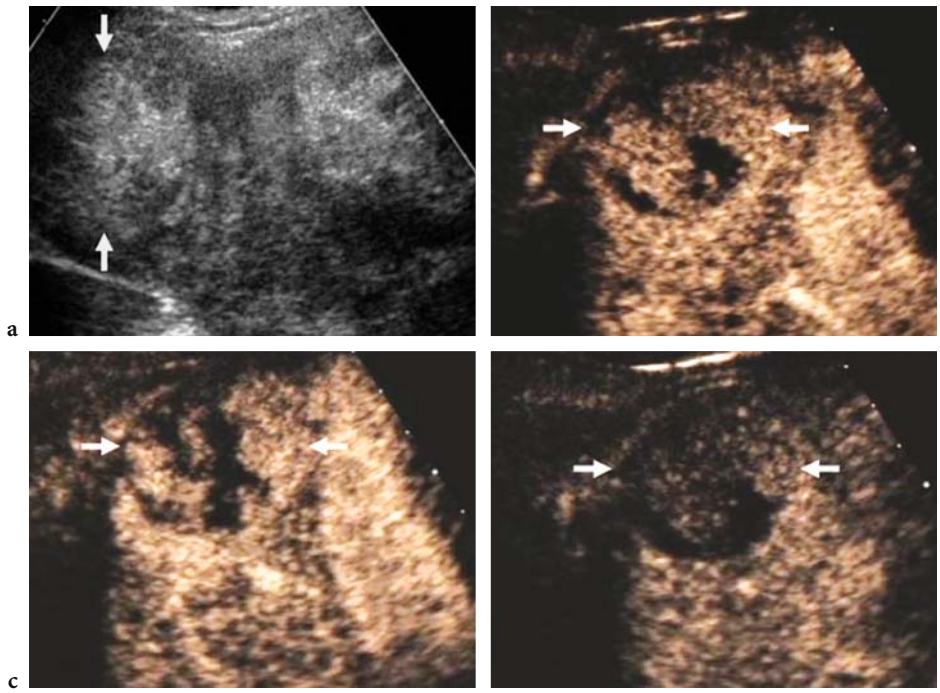

Fig. 11.30a–d. Large hepatocellular carcinoma that has a heterogeneous appearance on contrast-enhanced US and is hypoechoic during the late phase. Axial plane. **a** Baseline US. A heterogeneous lesion is identified. **b–d** Contrast-specific mode: Cadence Contrast Pulse Sequence (Siemens-Acuson, CA, USA) with low acoustic power after injection of sulfur hexafluoride-filled microbubbles. The carcinoma (*arrows*) presents diffuse and heterogeneous contrast enhancement during the arterial (**b**, 22 s after SonoVue injection) and the portal (**c**) phase and has a hypovascular appearance during the late phase (**d**) as compared to the adjacent liver parenchyma.

1994). Among nongastrointestinal malignancies, breast and lung cancers and melanoma are most likely to develop hepatic metastases. In comparison with the adjacent liver, metastases may present a hypovascular or, less frequently, a hypervascular pattern.

Multimodality imaging – US and color Doppler US. Metastases may display a variety of patterns on baseline US. Lesions may appear solid or cystic, with a hyper-, iso-, or hypoechoic pattern in comparison to the adjacent liver. Calcifications with posterior acoustic shadowing are typically observed in metastases from colorectal carcinoma. The peripheral hypoechoic halo, caused by the adjacent compressed liver parenchyma, is the most typical feature on baseline US, allowing characterization of metastases in most cases. On baseline color Doppler US, hypervascular metastases show a similar degree of hypervascularity to fibrous nodular hyperplasia and hepatocellular carcinoma (Harvey and Albrecht 2001).

Multimodality imaging - CT. Metastases typically appear hypodense on nonenhanced scan and present a persistent hypodense appearance on arterial, portal, and late phase scans (Nino-Murcia et al. 2000). After the injection of iodinated contrast agents, hypervascular metastases usually appear hyperdense (Oliver et al. 1997) compared to the adjacent liver in the arterial phase and hypodense in the late phase.

Multimodality imaging - RM. The most typical pattern is hypointensity on T1-weighted images and hyperintensity on T2-weighted images. Metastases appear hypointense on late phase images 1 h after the injection of liver-specific Gd-BOPTA.

Contrast-enhanced US. After microbubble agent administration, hypovascular metastases display absent (Figs. 11.32, 11.33) or dotted enhancement. Evidence of peripheral rim-like enhancement may be obtained during the arterial phase (Fig. 11.33), and fades at the beginning of the portal phase.

Diffusely enhancing hypervascular metastases appear hyperechoic (Harvey and Albrecht 2001; Quaia et al. 2004) from 20 to 30 s after microbubble injection (Figs. 11.34, 11.35), with evidence of a

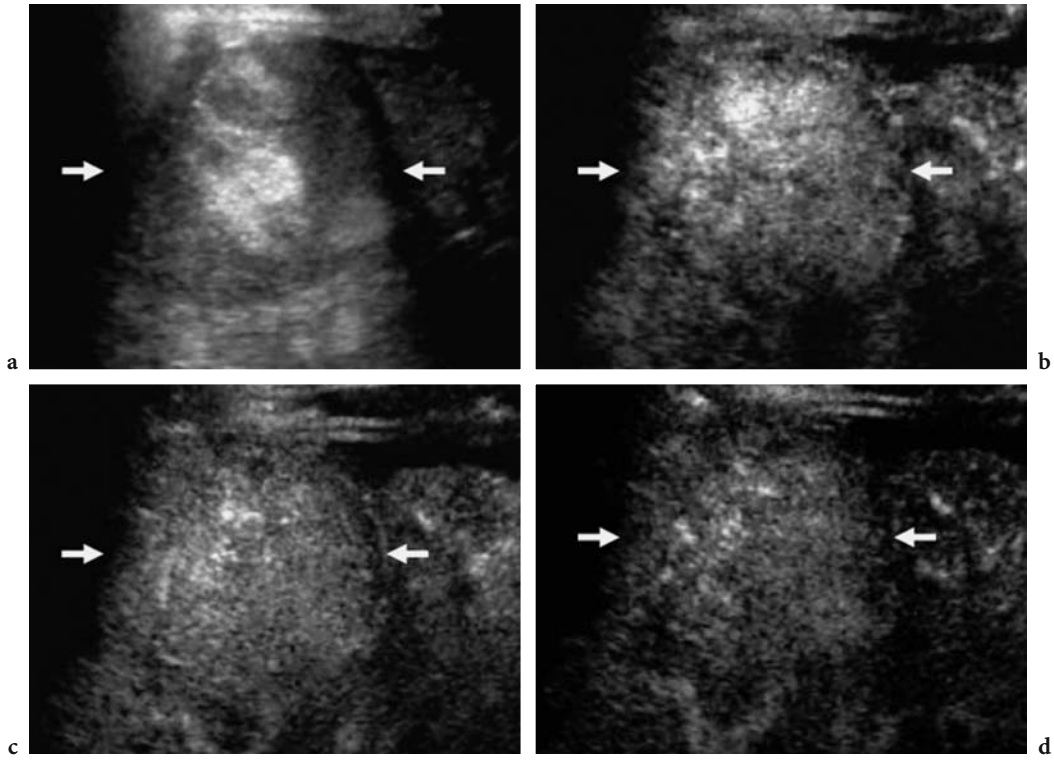

Fig. 11.31a–d. Large hepatocellular carcinoma that has a heterogeneous appearance on contrast-enhanced US and is isoechoic during the late phase. Axial plane. **a** Baseline US. A heterogeneous lesion is identified. **b–d** Contrast-specific mode: Pulse Inversion Mode (Philips-ATL, WA, USA) with low acoustic power after the injection of sulfur hexafluoride-filled microbubbles. The carcinoma (*arrows*) presents diffuse and heterogeneous contrast enhancement during the arterial (**b**, 22 s after SonoVue injection) and portal (**c**) phases and has an isovascular appearance in the late phase (**d**) as compared to the adjacent liver parenchyma.

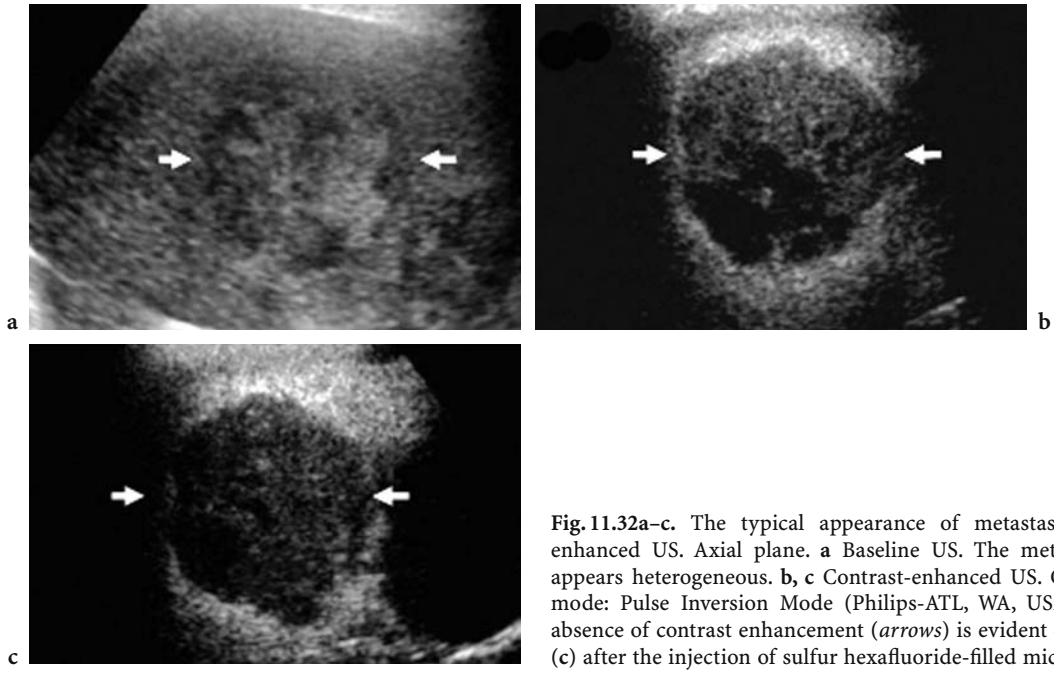

Fig. 11.32a–c. The typical appearance of metastasis on contrast-enhanced US. Axial plane. **a** Baseline US. The metastasis (*arrows*) appears heterogeneous. **b, c** Contrast-enhanced US. Contrast-specific mode: Pulse Inversion Mode (Philips-ATL, WA, USA). A persistent absence of contrast enhancement (*arrows*) is evident 40 s (**b**) and 90 s (**c**) after the injection of sulfur hexafluoride-filled microbubbles.

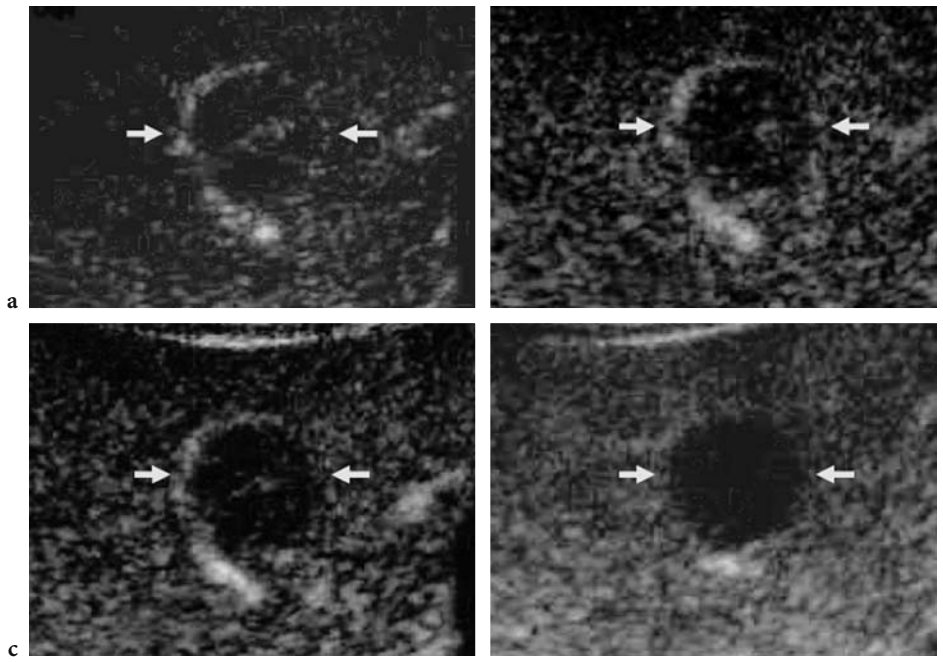

Fig. 11.33a–d. The typical appearance of metastasis on contrast-enhanced US. Axial plane. Contrast-enhanced US. Contrast-specific mode: Contrast Tuned Imaging (Esaote, Genoa, Italy) after the injection of sulfur hexafluoride-filled microbubbles. Persistent peripheral rim-like contrast enhancement (*arrows*) is evident during the arterial (**a**) and the portal phase (**b, c**), with a hypoechoic appearance in the late phase (**d**).

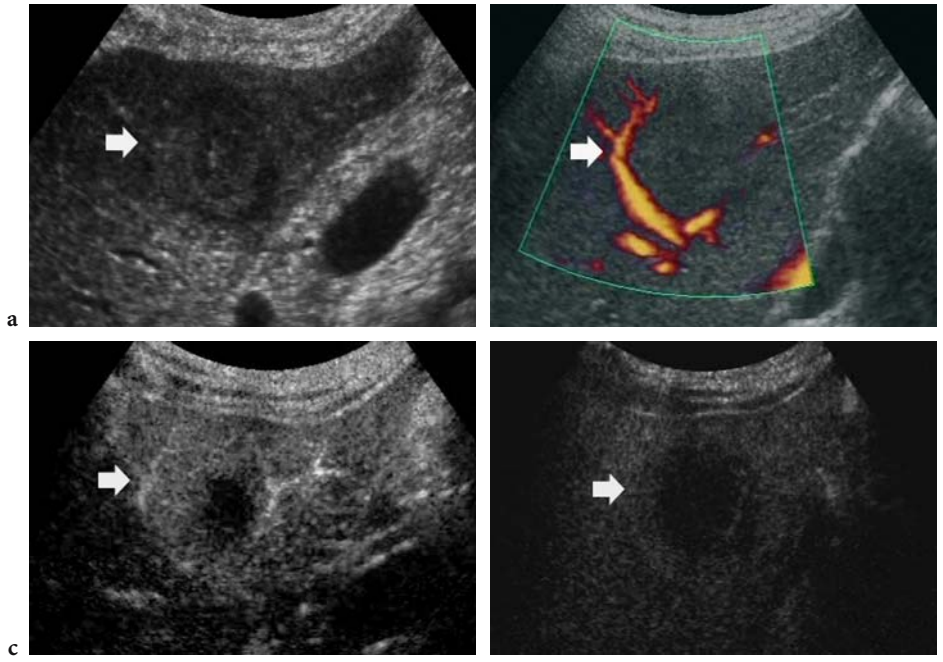

Fig. 11.34a–d. The typical appearance of metastasis on contrast-enhanced US. Axial plane. Baseline US (**a**) reveals a heterogeneous lesion (*arrow*) with a hypovascular appearance on power Doppler (**b**). **c, d** Contrast-enhanced US. Contrast-specific mode: Pulse Inversion Mode (Philips-ATL, WA, USA) with low acoustic power after the injection of sulfur hexafluoride-filled microbubbles. Persistent peripheral contrast enhancement (*arrow*) is identified during the arterial phase, with evidence of diffuse contrast enhancement sparing a peripheral portion of the lesion during the portal phase (**c**). The lesion appears hypoechoic (*arrow*) in the late phase (**d**).

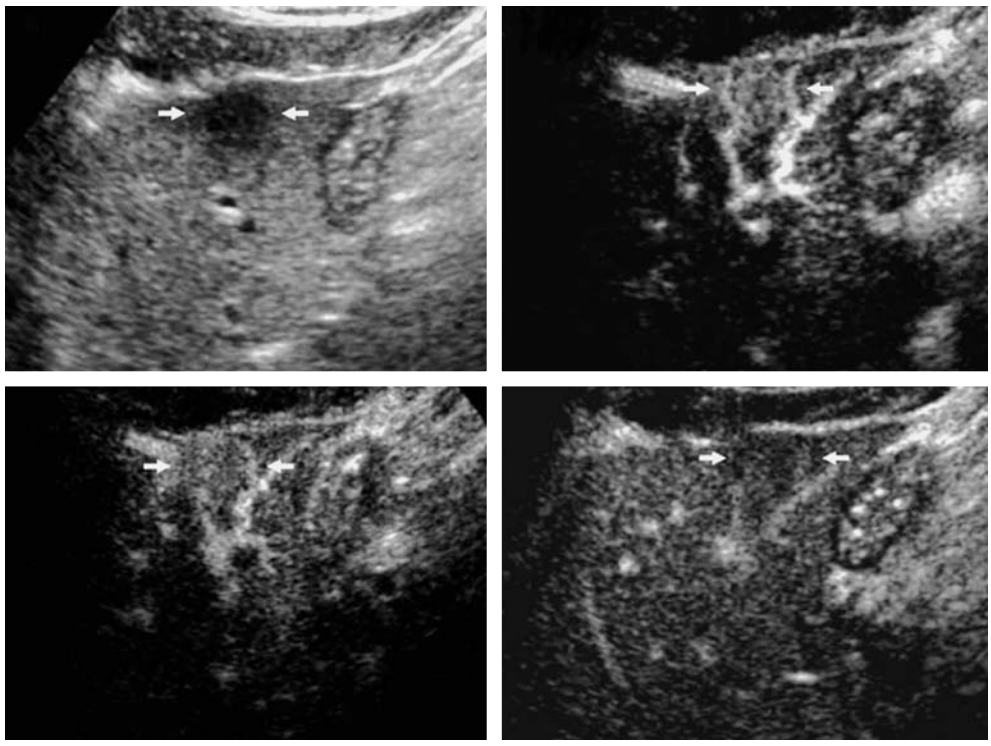

Fig. 11.35a–d. Metastasis. Diffuse contrast enhancement on contrast-enhanced US. Axial plane. **a** Baseline US. A hypoechoic lesion (*arrows*) with smooth margins is identified in the left lobe of the liver. **b–d** Contrast-enhanced US. Contrast-specific mode: Pulse Inversion Mode (Philips-ATL, WA, USA) after the injection of sulfur hexafluoride-filled microbubbles. Diffuse contrast enhancement is evident during the arterial (**b**) and the portal (**c**) with a hypoechoic appearance in the late phase (**d**).

peripheral hyperechoic rim in the majority of cases from 40 to 60 s after injection.

During the portal and late phases all metastases appear as hypoechoic defects in the liver with indistinct margins and improved conspicuity in comparison to the baseline scan (Heckemann et al. 2000; Meuwly et al. 2003); as a consequence, detectability is enhanced.

11.4.3 Intrahepatic Cholangiocellular Carcinoma

Epidemiology and histopathologic features. Cholangiocellular carcinoma is the most common tumor of the bile ducts and its incidence is increasing. Predisposing factors include sclerosing cholangitis, ulcerative colitis, choledochal cysts, Caroli's disease, parasitic infections (*Clonorchis sinensis*), and chemicals.

Multimodality imaging. Intrahepatic (or peripheral) cholangiocellular carcinoma demonstrates typically heterogeneous contrast enhancement at different dynamic phases. Rim-like contrast enhancement around the tumor during the arterial phase, and centripetal filling of contrast material during the equilibrium phase, due to the leak in the fibrous stroma of the tumour, are characteristic appearances on contrast-enhanced CT (Berland et al. 1989; Lee et al. 2001).

Contrast-enhanced US. Intrahepatic cholangiocellular carcinoma displays a persistent heterogeneous hypoechoic appearance (Khalili et al. 2003) (Fig. 11.36). In the arterial phase, ring enhancement appears in the periphery of the tumor and lasts until the portal phase in the majority of cholangiocellular carcinomas. In the late phase, absence of contrast enhancement has been observed (Tanaka et al. 2001). The absence of centripetal filling is due to the pure intravascular permanence of microbubbles.

11.4.4 Other Malignant Focal Liver Lesions

Other malignant focal liver lesions may be identified and scanned after the injection of microbubble-based agents, such as epithelioid hemangioendothelioma (Ghekiere et al. 2004), hepatic lymphoma.

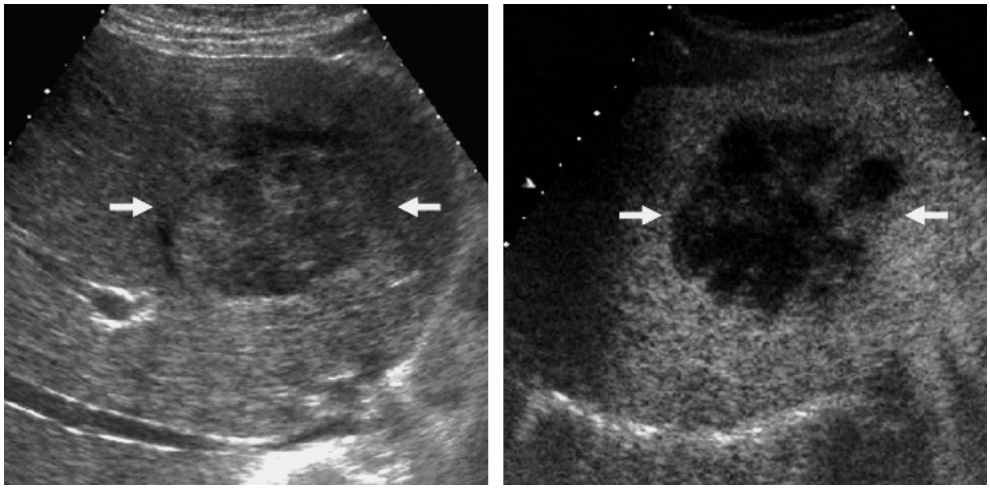

Fig. 11.36a,b. The typical appearance of cholangiocellular carcinoma on contrast-enhanced US. **a** At baseline US a heterogeneous hypoechoic lesion (*arrows*) is identified in the liver. **b** After microbubble injection, during the late phase the lesion appears hypoechoic compared to the adjacent liver.

The appearance of epithelioid hemangioendothelioma on contrast-enhanced US has recently been described (Quaia et al. 2004). Epithelioid hemangioendothelioma is a rare, low-grade malignant neoplasm of vascular origin composed of epithelioid-appearing endothelial cells. It should not be confused with infantile hemangioendothelioma, which regresses spontaneously. The tumor is characteristically composed of a fibrotic hypovascular central core, a peripheral hyperemic rim, and a further peripheral nonenhancing rim corresponding to a vascular zone between the lesion and the adjacent liver (Ghekiere et al. 2004). After microbubble injection it displays persistent diffuse contrast enhancement, with a hyperechoic appearance (Fig. 11.37), including during the late phase.

Hepatic lymphoma reveals hypovascular appearance at late phase (von Hersay 2004a,b).

11.5 Clinical Results

The development and clinical introduction of microbubble contrast agents has had a particular impact on the detection and differential diagnosis of liver tumors (Cosgrove and Blomley 2004). Malig-

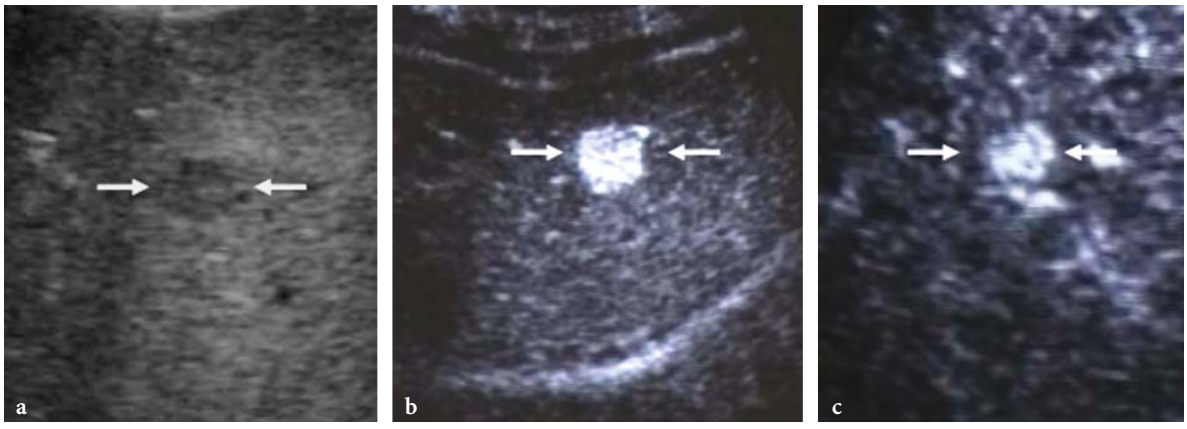

Fig. 11.37a–c. Epithelioid hemangioendothelioma on contrast-enhanced US. **a** On baseline US a hypoechoic lesion (*arrows*) is identified in the liver. **b, c** Contrast-specific mode: Pure Harmonic Detection (Aloka, Tokyo, Japan) with low acoustic power after the injection of sulfur hexafluoride-filled microbubbles. After microbubble injection, during the arterial phase (**b**) the lesion presents diffuse contrast enhancement (*arrows*) that persists into the late phase (**c**).

nancies typically show a low echo signal intensity during the late phase, regardless of whether they are hyper- or hypovascular in terms of their arterial supply. In addition, the arterial supply can be depicted in real time by using the low acoustic power mode, which allows differentiation of most benign masses from each other and from malignancies, and thus improves specificity.

Tanaka et al. (2001) reported that when a diffuse or heterogeneous mosaic enhancement pattern (arterial phase) and/or reticular enhancement (late phase) was regarded as indicative of hepatocellular carcinoma after Levovist injection, the sensitivity, specificity, and positive predictive value of contrast-enhanced US were 92%, 96%, and 96%, respectively. If peripheral rim-like enhancement (arterial to portal phase) or absence of enhancement (late phase) or both were regarded as positive findings for cholangiocellular carcinoma or metastasis, the sensitivity, specificity, and positive predictive value were 90%, 95%, and 88%, respectively. If peripheral nodular enhancement (portal phase) was regarded as a positive finding for hemangioma, the sensitivity, specificity, and positive predictive value were 60%, 100%, and 100%, respectively.

A recent study (von Herbay et al. 2002) found that, compared with baseline US, contrast-enhanced US after Levovist injection improved the sensitivity for the discrimination of malignant versus benign liver lesions from 85% to 100%, and the specificity from 30% to 63%. Receiver operating characteristic analysis revealed a significant improvement in this discrimination [area under curve (A_z)=0.692±0.065 on baseline US, A_z=0.947±0.037 on contrast-enhanced US, p<0.001). All lesions that had homogeneous enhancement in the late phase of Levovist enhancement were benign.

By classifying focal liver lesions with an isoechoic or hyperechoic appearance relative to the adjacent liver during the late phase as suggestive of benignity and hypoechoic lesions as suggestive of malignancy, Nicolau et al. (2003b) were able to differentiate between malignant and benign focal liver lesions with an accuracy of 86.5%.

Quaia et al. (2004) found similar results in the discrimination of benign from malignant lesions by using contrast-enhanced US after SonoVue injection: the hypoechoic appearance in the late phase was found to be the most typical feature of malignancies. Benign lesions display persistent microbubble uptake while malignant lesions show microbubble washout and lower microbubble uptake compared to the adjacent liver during the late phase (Blomley et al. 2001; Albrecht et al. 2003; Nicolau et al. 2003a,b; Quaia et al. 2004). In the same study by Quaia et al. (2004), two off-site readers retrospectively assessed each focal liver lesion and reached a conclusion as to its malignant or benign nature based on the appearance of the lesion before and after microbubble injection. After the additional review of contrast-enhanced scans, diagnostic performance was improved for both readers in about two-thirds of lesions, through the achievement of either correct diagnosis or greater diagnostic confidence. After microbubble injection about 7% of the lesions remained indeterminate and were characterized by histologic analysis of the biopsy or surgical specimen (Quaia et al. 2004).

The two other principal imaging modalities for the evaluation of focal liver lesions are CT and MR imaging. The more suitable imaging procedure for characterization of focal liver lesions that remain indeterminate after microbubble injection is probably contrast-enhanced MR with gadolinium chelates, iron oxide compounds, or manganese chelates. This allows both dynamic and tissue-specific characterization with a better diagnostic performance (85–95%: Grazioli et al. 2001a,b; Oudkerk et al. 2002; Kim et al. 2004b) than multiphase contrast-enhanced CT (68–91%: van Leeuwen et al. 1996; Oudkerk et al. 2002; Kamel et al. 2003).

11.6 When Should Microbubble-Based Agents Be Employed?

Baseline US and color Doppler US are effective in characterizing incidental focal liver lesions as benign or malignant in the normal liver in about 40–50% of cases (Nino-Murcia et al. 1992; Reinhold et al. 1995; Lee et al. 1996). This is because typical hemangiomas, focal nodular hyperplasias, and metastases often display a typical appearance on gray-scale US or characteristic vessel architecture on color Doppler US. In the remaining 50–60% of cases, microbubble-based agents should be employed to improve the characterization of focal liver lesions through the identification of typical contrast enhancement patterns (Tables 11.1 and 11.2). In about 10% of cases, focal liver lesions remain indeterminate even after microbubble injection; contrast-enhanced MR imaging should then be employed, followed when necessary by US-guided biopsy.

The possible diagnosis of hepatocellular carcinoma should be considered for each incidental focal liver lesion identified in the cirrhotic liver. Baseline

Table 11.1. Benign Lesion Summary of the baseline gray-scale and color Doppler US findings and of contrast enhancement patterns after microbubbles injection

Baseline		**Contrast Enhancement patterns ***		
Gray scale US	**color Doppler US**	**Arterial phase**	**Portal phase**	**Late phase**
Typical hemangioma Hyperechoic, homogenous, sharp margins and possible posterior enhancement. Frequent sub-caspular location. Multiple in 10% of cases	Extralesional feeding vessels	Peripheral nodular enhancement	Slow centripetal progression of the enhancement leading to an iso- or hyperechoic appearance	Complete fill-in and hyperechoic or sometimes isoechoic appearance.
Atypical hemangioma Hyper-, iso-, hypoechoic or heterogeneous echogenicity with larger hypoechoic areas related to hemorrhage, thrombosis or necrosis.		No enhancement in case of completed thrombosis Diffuse enhancement (rapid fill-in) during arterial phase with hyperechoic appearance		Fill-in may be incomplete in case of thrombosis
Focal nodular hyperplasia Variable echogenicity (iso-, hypo-, hyperechoic or heterogeneious). Central scar may be visible as hypoechoic central area. Multiple in 20% of cases.	Spoke-whell shaped pattern consisting in central and radiating arterial vessels with high diastolic component compared to the systolic component. Large vessels may be present in the lesion periphery. Feeding artery may be present especially in small lesions	Spoke-whell shaped central enhancement. Radial vascular branches and peripheral vessel can be delineated. Diffuse contrast enhancement.	Iso- or hyperechoic	Iso- or hyperechoic. Evidence of the central scar with hypoechoic appearance
Hepatocellular adenomas Variable echogenicity (iso-, hypo-, hyperechoic; heterogeneous in larger lesions secondary to necrosis, hemorrhage or fibrosis). Pseudo-halo possible due to compression of adjacent parenchyma. Rarely isolated calcifications.	Large peripheral arteries and veins; prevalently venous vessels in the lesion center Feeding artery may be identified	Diffuse enhancement with homogeneous or heterogeneous appearance.	Homogeneous or heterogeneous appearance with hypoechoic areas in case of hemorrhage, necrosis or fibrosis	Homogeneous or heterogeneous appearance with hypoechoic areas in case of hemorrhage, necrosis or fibrosis
Macroregenerative or dysplastic nodule Predominantly hypoechoic but also hyperechoic or heterogeneous. Presence of liver cirrhosis as under-lying diseases.	No intralesional vessels	Absent or Dotted enhancement with hypoechoic or isoechoic appearance. Diffuse enhancement possible in dysplastic lesions	Isoechoic	Isoechoic
Focal fatty changes Often geometric/polygonal with sharp margins Hyperechoic with normal surrounding liver tissue Typically located near falciform ligament / antero-medial portion of Segment IV / hilar side of Segment IV / anterolateral portion of Segment III and/ or hepatic hilum.	No vascular abnormalities	Isoechoic	Isoechoic	Isoechoic
Focal fatty sparings Often geometric/polygonal with sharp margins Hypoechoic (surrounding liver tissue hyperechoic [fatty liver]) Typically located along the hepatic hilum and/or around the gallbladder and Segment IV.	No vascular abnormalities	Isoechoic	Isoechoic	Isoechoic

Table 11.2. Malignant Lesions

Baseline		Contrast enhancement patterns *		
Gray scale US	**color Doppler US**	**Arterial phase**	**Portal phase**	Late phase
Hepatocellular carcinomas				
Small lesions (< 3cm): prevalently hypoechoic. Sometimes hyperechoic depending on fat content. Isoechoic appearance is rare	Intratumoral arterial vessels depending on degree of differentiation with irregular tortous tumor vessels.	Diffuse homogeneous or heterogeneous enhancement, often with delineation of feeding peripheral and intratumoral vessels.	Iso- or hypoechoic; generally contrast washout begins. Heterogeneous appearance possible	Prevalently hypoechoic Isoechoic appearance.
Large lesions (>3cm): heterogeneous. Sometimes evidence of hypoechoic rim	I rregular tortous peritumoral vessels.	Dotted enhancement.		
	Basket pattern consisting in irregular peripheral arterial vessels with centripetal intratumoral branches	Heterogeneous appearance in large lesions, if necrotic or hemorrhagic areas are present		
Intrahepatic cholangiocarcinoma				
Heterogeneous with diffuse and infiltrating margins	Intratumoral vessels often at the edge of the tumor	Heterogeneous enhancement	Heterogeneous enhancement	Hypoechoic
Segmental biliary dilatation	Poorly vascularized lesion	Peripheral rim-like enhancement		
Hypervascular Metastases				
Variable echogenicity: prevalently hypoechoic (sometimes cystic). frequently isoechoic and hyperechoic. Intratumoral calcifications are possible. Presence of a peripheral hypoechoic halo	Tumor vessels are often restricted to the periphery of the lesion	Diffuse Heterogeneous appearance especially in large lesions and if necrotic areas are present	Iso- or hypoechoic due to rapid contrast washout. Rim-like peripheral enhancement may persist.	Hypoechoic
Hypovascular Metastases Variable echogenicity: prevalently hypoechoic (sometimes cystic). frequently isoechoic and hyperechoic. Presence of a peripheral hypoechoic halo.	Peripheral vessels	Absent or dotted contrast enhancement with hypoechoic appearance	Hypoechoic	Hypoechoic

Note: Different baseline appearance and contrast enhancement patterns of benign and malignant focal liver lesions.
* Echogenicity is compared to the adjacent liver parenchyma.
hyperechoic = hypervascular
hypoechoic = hypovascular
isoechoic = isovascular

US and color Doppler US have a very low diagnostic accuracy with respect to focal liver lesions in the cirrhotic liver (Nino-Murcia et al. 1992), and microbubble-based agents have to be employed in all cases except those in which a large lesion has an overtly malignant appearance on the baseline scan. Approximately 40–50% of lesions in the cirrhotic liver remain indeterminate or present an atypical appearance after microbubble injection (Quaia et al. 2004), and contrast-enhanced CT or MR imaging should then be employed. Differentiation of high-grade dysplastic nodules from hepatocellular carcinoma is often not possible using imaging modalities, necessitating US-guided biopsy.

The Efsumb Study Group (2004) recently proposed guide-lines for the employment of microbubbles in liver tumors.

References

Albrecht T, Oldenburg A, Hohmann J et al (2003) Imaging of liver metastases with contrast-specific low-MI real time ultrasound and SonoVue. Eur Radiol 13 [Suppl 3]:N79-N86

Alpers DH, Isselbacher KJ (1975) Fatty liver: biochemical and clinical aspects. In: Schieff L (ed) Diseases of the liver. Lippincott, Philadelphia, pp 815-832

Baker MK, Wenker JC, Cockerill EM, Ellis JH (1985) Focal fatty infiltration of the liver: diagnostic imaging. RadioGraphics 5:923-929

Baron RL, Peterson MS (2001) Screening the cirrhotic liver for hepatocellular carcinoma with CT and MR imaging: opportunities and pitfalls. Radiographics 21:S117-S132

Bartolozzi C, Lencioni R, Paolicchi A et al (1997) Differentiation of hepatocellular adenoma and focal nodular hyperplasia of the liver: comparison of power Doppler imaging and conventional color Doppler sonography. Eur Radiol 7:1410-1415

Berland L, Lee JKT, Stanley RJ (1989) Liver and biliary tract. In: Lee JKT, Sagel SS, Stanley RJ (eds) Computed body tomography with MRI correlation, 2nd edn. Raven, New York, pp 593-659

Bertolotto M, Dalla Palma L, Quaia E, Locatelli M (2000) Characterization of unifocal liver lesions with pulse inversion harmonic imaging after Levovist injection: preliminary results. Eur Radiol 9:1369-1376

Blachar A, Federle MP, Ferris JV et al (2002) Radiologists' performance in the diagnosis of liver tumors with central scars by using specific CT criteria. Radiology 223:532-539

Blomley MJK, Albrecht T, Cosgrove DO et al (1998) Stimulated acoustic emission in liver parenchyma with Levovist. Lancet 351:568-569

Blomley MJ, Albrecth TA, Cosgrove DO et al (1999) Improved detection of liver metastases with stimulated acoustic emission in late phase of enhancement with the US contrast agent SH U 508: early experience. Radiology 210:409-416

Blomley MJK, Sidhu PL, Cosgrove DO et al (2001) Do different types of liver lesions differ in their uptake of the microbubble contrast agent SH U 508A in the late liver phase? Early experience. Radiology 220:661-667

Bluemke D, Weber TM, Rubin D et al (2003) Hepatic MR imaging with ferumoxides: multicenter study of safety and effectiveness of direct injection protocol. Radiology 228:457-464

Brancatelli G, Federle MP, Blachar A, Grazioli L (2001a) Hemangioma in the cirrhotic liver: diagnosis and natural history. Radiology 219:69-74

Brancatelli G, Federle MP, Grazioli L et al (2001b) Focal nodular hyperplasia: CT findings with emphasis on multiphasic helical CT in 78 patients. Radiology 219:61-68

Brancatelli G, Federle MP, Grazioli L, Carr BI (2002a) Hepatocellular carcinoma in noncirrhotic liver: CT, clinical, and pathologic findings in 39 US residents. Radiology 222:89-94

Brancatelli G, Federle MP, Grazioli L et al (2002b) Benign regenerative nodules in Budd-Chiari syndrome and other vascular disorders of the liver: radiologic–pathologic and clinical correlation. Radiographics 22:847-862

Brannigan M, Burns PN, Wilson SR (2004) Blood flow patterns in focal liver lesions at microbubble-enhanced US. Radiographics 24:921-935

Brawer MK, Austin GE, Lewin JK (1980) Focal fatty change of the liver, a hitherto poorly recognized entity. Gastroenterology 78:247-252

Bryant TH, Blomley MJ, Albrecht T et al (2004) Improved characterization of liver lesions with liver-phase uptake of liver specific microbubbles: prospective multicenter trials. Radiology 232:799-809

Burns PN, Powers JE, Simpson DH et al (1996) Harmonic imaging: principles and preliminary results. Clin Radiol 51(Suppl):50–55

Burns P, Wilson S, Simpson D (2000) Pulse inversion imaging of liver blood flow. Improved method for characterization focal masses with microbubble contrast. Invest Radiol 35:58-71

Chen RC, Chen WT, Tu HY et al (2002) Assessment of vascularity in hepatic tumours. Comparison of power Doppler sonography and intraarterial CO2-enhanced sonography. Am J Roentgenol 178:67-73

Chen WP, Chen JH, Hwang JI et al (1999) Spectrum of transient hepatic attenuation differences in biphasic helical CT. AJR Am J Roentgenol 172:419-424

Choi BI, Kim AY, Lee JY et al (2002) Hepatocellular carcinoma: contrast enhancement with Levovist. J Ultrasound Med 21:77-84

Claudon M, Tranquart F, Evans DH et al (2002) Advances in ultrasound. Eur Radiol 12:7-18

Colagrande S, Politi LS, Messerini L et al (2003) Solitary necrotic nodule of the liver: imaging and correlation with pathologic features. Abdom Imaging 28:41-44

Correas JM, Burns PN, Lai X, Qi X (2000) Infusion versus bolus of an ultrasound contrast agent: in vivo dose-response measurements of BR1. Invest Radiol 35:72-79

Correas JM, Bridal L, Lesavre A et al (2001) Ultrasound contrast agents: properties, principles of action, tolerance, and artifacts. Eur Radiol 11:1316-1328

Cosgrove DO, Blomley MJK (2004) Liver tumors: Evaluation with contrast-enhanced ultrasound. Abdom Imaging 29:446-454

Cosgrove DO, Blomley MJK, Eckersley RJ, Harvey C (2002) Innovative contrast specific imaging with ultrasound. Electromedica 70:147-149

De Luca M, Luigi B, Formisano C et al (2000) Solitary necrotic nodule of the liver misinterpreted as malignant lesion: considerations on two cases. J Surg Oncol 74:219-222

Dill-Macky M, Burns P, Khalili K, Wilson S (2002) Focal hepatic masses: enhancement patterns with SH U 508 A and pulse inversion US. Radiology 222:95-102

Ebara M, Ohto M, Shinagawa T et al (1986) Natural history of minute hepatocellular carcinoma smaller than three centimetres complicating cirrhosis. A study of 22 patients. Gastroenterology 90:289-298

Edmondson HA (1958) Tumors of the liver and intrahepatic bile ducts. Atlas of tumor pathology. Armed Forces Institute of Pathology, Washington DC

Efsumb Study Group (2004) Guidelines for the use of contrast agents in ultrasound. Ultraschall Med 25:249–256

Ferrucci JT (1994) Liver tumour imaging. Current concepts. Radiol Clin North Am 32:39-54

Furuse J, Nagase M, Ishii H, Yoshino M (2003) Contrast enhancement patterns of hepatic tumours during the vascular phase using coded harmonic imaging and Levovist to differentiate hepatocellular carcinoma from other focal lesions. Br J Radiol 76:385-392

Gatenby JC, Hoddinott JC, Leeman S (1989) Phasing out speckle. Phys Med Biol 34:1683-1689

Ghekiere O, Weynand B, Pieters T, Coche E (2004) Epithelioid haemangioendothelioma. Eur Radiol 14:1134-1137

Giorgio A, Ferraioli G, Tarantino L et al (2004) Contrast-enhanced sonographic appearance of hepatocellular carcinoma in patients with cirrhosis: comparison with contrast-enhanced helical CT appearance. AJR Am J Roentgenol 183:1319-1326

Golli M, van Nhieu JT, Mathieu D et al (1994) Hepatocellular adenoma: color Doppler US and pathologic correlations. Radiology 190:741-744

Gonzàlez-Anòn M, Cervera-Deval J, Garcia-Vila JH et al (1999) Characterization of solid liver lesions with color and pulsed Doppler imaging. Abdom Imaging 24:137-143

Gramiak R, Shah PM (1968) Echocardiography of the aortic root. Invest Radiol 3:356-366

Grazioli L, Federle MP, Brancatelli G (2001a) Hepatic adenomas: imaging and pathologic findings. Radiographics 21:877-892

Grazioli L, Morana G, Federle MP et al (2001b) Focal nodular hyperplasia: morphologic and functional information from MR imaging with gadobenate dimeglumine. Radiology 221:731-739

Halvorsen RA, Korobkin M, Ram PC, Thompson WM (1982) CT appearance of focal fatty infiltration of the liver. Am J Roentgenol 139:277-281

Harvey CJ, Albrecht T (2001) Ultrasound of focal liver lesions. Eur Radiol 11:1578-1593

Hayashi M, Matsui O, Ueda K et al (1999) Correlation between the blood supply and grade of malignancy of hepatocellular nodules associated with liver cirrhosis: evaluation by CT during intraarterial injection of contrast medium. AJR Am J Roentgenol 172:969-976

Hayashi M, Matsui O, Ueda K et al (2002) Progression to hypervascular hepatocellular carcinoma: correlation with intranodular blood supply evaluated with CT during intraarterial injection of contrast material. Radiology 225:143-149

Hauff P, Fritsch T, Reinhardt M et al (1997) Delineation of experimental liver tumors in rabbits by a new ultrasound contrast agent and stimulated acoustic emission. Invest Radiol 32:94-99

Heckemann R, Cosgrove DO, Blomley MJK et al (2000) Liver lesions: intermittent second-harmonic gray-scale US can increase conspicuity with microbubble contrast material-early experience. Radiology 216:592-596

Hirohashi S, Ueda K, Uchida H et al (2000) Nondiffuse fatty change of the liver: discerning pseudotumor on MR images enhanced with ferumoxides - initial observations. Radiology 217:415-420

Hohmann J, Skrok J, Puls R, Albrecth T (2003) Characterization of focal liver lesions with contrast-enhanced low MI real time ultrasound and SonoVue. Rofo Rontgenstr Fortschr 176:835-843

Hosten N, Puls R, Bechstein WO, Felix R (1999a) Focal liver lesions: Doppler ultrasound. Eur Radiol 9:428-435

Hosten N, Puls R, Lemke AJ et al (1999b) Contrast enhanced power Doppler sonography: improved detection of characteristic flow patterns in focal liver lesion. J Clin Ultrasound 27:107-115

Hussain SH, Zondervan PE, IJzermans JNM et al (2002) Benign versus malignant hepatic nodules: MR imaging findings with pathologic correlation. Radiographics 22:1023-1036

Ichikawa T, Federle MP, Grazioli L et al (1999) Fibrolamellar hepatocellular carcinoma: imaging and pathologic findings in 31 recent cases. Radiology 213:352-361

Ichikawa T, Federle MP, Grazioli L, Nalesnik M (2000) Hepatocellular adenoma: multiphasic CT and histopathologic findings in 25 patients. Radiology 214:861-868

Isozaki T, Numata K, Kiba T (2003) Differential diagnosis of hepatic tumors by using contrast enhancement patterns at US. Radiology 229:798-805

Jespersen SK, Wilhjelm JE, Sillesen H (1998) Multiangle compound imaging. Ultrason Imaging 20:81-102

Leen E, Angerson WJ, Yarmenitis S et al (2002) Multi-centre study evaluating the efficacy of SonoVue (BR1), a new ultrasound contrast agent in Doppler investigation of focal hepatic lesions. Eur J Radiol 41:200-206

Kamel IR, Choti MA, Horton KM et al (2003) Surgically staged focal liver lesions: accuracy and reproducibility of dual-phase helical CT for detection and characterization. Radiology 227:752-757

Kane AG, Redwine MD, Cossi AF (1993) Characterization of focal fatty change in the liver with a fat-enhanced inversion recovery sequenze. J Magn Reson Imaging 3:581-586

Karhunen PJ (1986) Benign hepatic tumors and tumor-like conditions in men. J Clin Pathol 39:183-188

Khalili K, Metser U, Wilson SR (2003) Hilar biliary obstruction: preliminary results with Levovist-enhanced sonography. Am J Roentgenol 180:687-693

Kim EA, Yoon KH, MD, Lee YH (2003) Focal hepatic lesions: contrast-enhancement patterns at pulse-inversion harmonic US using a microbubble contrast agent. Korean J Radiol 4:224-233

Kim HC, Kim TK, Sung KB et al (2002) CT during hepatic arteriography and portography: an illustrative review. Radiographics 22:1041-1051

Kim MG, Kim JH, Chung JJ (2003) Focal hepatic lesions: detection and characterization with combination Gadolinium- and Superparamagnetic iron oxide-enhanced MR imaging. Radiology 228:719-726

Kim TK, Han JK, Kim AY, Choi BI (1999) Limitations of characterization of hepatic hemangiomas using an ultrasound contrast agent (Levovist) and power Doppler ultrasound. J Ultrasound Med 18:737-743

Kim TK, Choi BI, Han JK et al (2000) Hepatic tumours: contrast agent-enhancement patterns with pulse inversion harmonic US. Radiology 216:411-417

Kim KW, Choi BI, Park SH et al (2003) Hepatocellular carcinoma: assessment of vascularity with single-level dynamic ultrasonography during the arterial phase. J Ultrasound Med 22:887-896

Kim KW, Choi BI, Park SH et al (2004a) Pyogenic hepatic abscesses: distinctive features from hypovascular hepatic malignancies on contrast-enhanced ultrasound with SH U 508A; early experience. Ultrasound Med Biol 30:725-733

Kim KW, Kim AY, Kim TK et al (2004b) Small (≤2 cm) hepatic lesions in colorectal cancer patients: detection and characterization on mangafodipir trisodium-enhanced MRI. AJR Am J Roentgenol 182:1233-1240

Kindberg GM, Tolleshaug H, Roos N, Skotland T (2003) Hepatic clearance of Sonazoid perfluorobutane microbubbles by Kupffer cells does not reduce the ability of liver to phagocytose or degrade albumin microspheres. Cell Tissue Res 312:49-54

Kirchin MA, Pirovano GP, Spinazzi A (1998) Gadobenate dimeglumine (Gd-BOPTA): an overview. Invest Radiol 33:798-809

Kissin CM, Bellamy EA, Cosgrove DO et al (1986) Focal sparing in fatty infiltration of the liver. Br J Radiol 59:25-28

Koda M, Matsunaga Y, Ueki M et al (2004) Qualitative assessment of tumour vascularity in hepatocellular carcinoma by contrast-enhanced coded ultrasound: comparison with arterial phase of dynamic CT and conventional color/power Doppler ultrasound. Eur Radiol 14:1100-1108

Koea J, Taylor G, Miller M et al (2003) Solitary necrotic nodule of the liver: a riddle that is difficult to answer. J Gastroint Surg 7:627-630

Kudo M, Tomita S, Tochio H et al (1992) Small hepatocellular carcinoma: diagnosis with US angiography with intraarterial CO2 microbubbles. Radiology 182:155-160

Larcos G, Sorokopud H, Berry G, Farrell GC (1998) Sonographic screening for hepatocellular carcinoma in patients with chronic hepatitis or cirrhosis: an evaluation. Am J Roentgenol 171:433-435

Lee MG, Auh YH, Cho KS et al (1996) Color Doppler flow imaging of hepatocellular carcinomas. Comparison with metastatic tumors and hemangiomas by three step grading color hues. Clin Imaging 20:199-203

Lee JY, Choi BI, Han JK et al (2002) Improved sonographic imaging of hepatic hemangioma with contrast-enhanced coded harmonic angiography: comparison with MR imaging. Ultrasound Med Biol 28:287-295

Lee KH, Choi BI, Kim KW et al (2003) Contrast-enhanced dynamic ultrasonography of the liver: optimization of hepatic arterial phase in normal volunteers. Abdom Imaging 28:652-656

Lee WJ, Lim HK, Jang KM (2001) Radiologic spectrum of cholangiocarcinoma: emphasis on unusual manifestations and differential diagnoses. Radiographics 21:S97-S116

Lencioni R, Pinto F, Armillotta N, Bartolozzi C (1996) Assessment of tumor vascularity in hepatocellular carcinoma: comparison of power Doppler US and color Doppler US. Radiology 201:353-358

Lim JH, Cho JM, Kim EY, Park CK (2000) Dysplastic nodules in liver cirrhosis: evaluation of hemodynamics with CT during arterial portography and CT hepatic arteriography. Radiology 214:869-874

Longchampt E, Patriarche C, Fabre M (2000) Accuracy of cytology vs microbiopsy for the diagnosis of well-differentiated hepatocellular carcinoma and macroregenerative nodule. Definition of standardized criteria from a study of 100 cases. Acta Cytol 44:515-523

Mathieu D, Bruneton JN, Drouillard J et al (1986) Hepatic adenomas and focal nodular hyperplasia: dynamic CT study. Radiology 160:53-58

Matsui O, Kadoya M, Kameyama T et al (1991) Benign and malignant nodules in cirrhotic liver: distinction based on blood supply. Radiology 178:493-497

McLarney JK, Rucker PT, Bender GN et al (1999) Fibrolamellar carcinoma of the liver: radiologic–pathologic correlation. Radiographics 19:453-471

Merritt CR, Forsberg F, Shi WT et al (2000) The mechanical index: an inappropriate and misleading indicator for destruction of ultrasound microbubble contrast agents. Radiology 217:395

Meuwly JY, Schnyder P, Gudinchet F, Denys AL (2003) Pulse-inversion harmonic imaging improves lesion conspicuity during US-guided biopsy. J Vasc Interv Radiol 14:335-341

Migaleddu V, Virgilio G, Turilli D et al (2004) Characterization of focal liver lesions in real time using harmonic imaging with high mechanical index and contrast agent Levovist. Am J Roentgenol 182:1505-1512

Mitchell DG, Rubin R, Siegelman ES et al (1991) Hepatocellular carcinoma within siderotic regenerative nodules: appearance as a nodule within a nodule on MR images. Radiology 178:101-103

Morel DR, Schwieger I, Hohn L et al (2000) Human pharmacokinetics and safety evaluation of SonoVue™, a new contrast agent for ultrasound imaging. Invest Radiol 35:80-85

Nicolau C, Catalá V, Brú C (2003a) Characterization of focal liver lesions with contrast-enhanced ultrasound. Eur Radiol 13 [Suppl 3]:N70-N78

Nicolau C, Catalá V, Vilana R (2003b) Is contrast-enhanced ultrasound late vascular phase evaluation enough to differentiate between benign and malignant focal liver lesions? (Abstract.) RSNA 2003, Scientific assembly and annual meeting program

Nicolau C, Catalá V, Vilana R et al (2004) Evaluation of hepatocellular carcinoma using SonoVue, a second generation ultrasound contrast agent: correlation with cellular differentiation. Eur Radiol 14:1092-1099

Nino-Murcia M, Ralls PW, Jeffrey RB Jr, Johnson M (1992) Color flow Doppler characterization of focal hepatic lesions. Am J Roentgenol 159:1195-1197

Nino-Murcia M, Olcott EW, Jeffrey RB et al (2000) Focal liver lesions: pattern-based classification scheme for enhancement at arterial phase. Radiology 215:746-751

Nomura Y, Matsuda Y, Yabuuchi I et al (1993) Hepatocellular carcinoma in adenomatous hyperplasia: detection with contrast-enhanced US with carbon dioxide microbubbles. Radiology 187:353-356

Numata K, Tanaka K, Mitsui K et al (1993) Flow characteristics of hepatic tumors at color Doppler sonography: correlation with arteriographic findings. Am J Roentgenol 160:515-521

Numata K, Tanaka K, Kiba T et al (2001) Contrast-enhanced wide-band harmonic gray-scale imaging of hepatocellular carcinoma: correlation with helical computed tomographic findings. J Ultrasound Med 20:89-98

Oliver JH III, Baron RL, Federle MP et al (1997) Hypervascular liver metastases: Do unenhanced CT and hepatic arterial phase CT images affect tumor detection? Radiology 205:709-715

Oudkerk M, Torres CG, Song B et al (2002) Characterization of liver lesions with mangafodipir trisodium-enhanced MR imaging: multicenter study comparing MR and dual-phase spiral CT. Radiology 223:517-524

Peterson MS, Baron RL, Marsh JW et al (2000) Pretransplantation surveillance for possible hepatocellular carcinoma in patients with cirrhosis: epidemiology and CT-based tumor detection rate in 430 cases with surgical pathologic correlation. Radiology 217:743-749

Quaia E, Bertolotto M, Dalla Palma L (2002a) Characterization of liver hemangiomas with pulse inversion harmonic imaging. Eur Radiol 12:537-544

Quaia E, Blomley MJK, Patel S et al (2002b) Initial observations on the effect of irradiation on the liver-specific uptake of Levovist. Eur J Radiol 41:192-199

Quaia E, Forgács B, Calderan L et al (2002c) Characterization of focal hepatic lesions in cirrhotic patients by pulse inversion harmonic imaging US contrast specific technique with levovist. Radiol Med 104:285-294

Quaia E, Bertolotto M, Calderan L et al (2003) US characterization of focal hepatic lesions with intermittent high acoustic power mode and contrast material. Acad Radiol 10:739-750

Quaia E, Calliada F, Bertolotto M et al (2004) Characterization of focal liver lesions by contrast-specific US modes and a sulfur hexafluoride-filled microbubble contrast agent: diagnostic performance and confidence. Radiology 232:420-430

Quiroga S, Sebastià C, Pallisa E et al (2001) Improved diagnosis of hepatic perfusion disorders: value of hepatic arterial phase imaging during helical CT. Radiographics 21:65-81

Reinhold C, Hammers L, Taylor CR et al (1995) Characterization of focal hepatic lesions with duplex sonography: findings in 198 patients. AJR Am J Roentgenol 164:1131-1135

Ros PR (1990) Computed tomography–pathologic correlations in hepatic tumors. In: Ferrucci JT, Mathiew DG (eds) Advances in hepatobiliary radiology. Mosby, St Louis, pp 75-108

Sandler MA, Petrocelli RD, Marks DS, Lopez R (1980) Ultrasonic features and radionuclide correlation in liver cell adenoma and focal nodular hyperplasia. Radiology 135:393

Schneider M, Arditi M, Barrau MB et al (1995) BR1: a new ultrasonographic contrast agent based on sulphur hexafluoride-filled microbubbles. Invest Radiol 30:451-457

Spinazzi A, Lorusso V, Pirovano G, Kirchin M (1999) Safety, tolerance, biodistribution, and MR imaging enhancement of the liver with gadobenate dimeglumine: results of clinical pharmacologic and pilot imaging studies in nonpatient and patient volunteers. Acad Radiol 6:282-291

Stevens WR, Gulino SP, Batts KP et al (1996) Mosaic pattern of hepatocellular carcinoma: histologic basis for a characteristic CT appearance. J Comput Assist Tomogr 20:337-342

Tanaka S, Kitamura T, Fujita M et al (1990) Color Doppler flow imaging of liver tumors. AJR Am J Roentgenol 154:509-514

Tanaka S, Kitamura T, Fujita M et al (1992) Small hepatocellular carcinoma: differentiation from adenomatous hyperplastic nodule with color Doppler flow imaging. Radiology 182:161-165

Tanaka S, Ioka T, Oshikawa O et al (2001) Dynamic sonography of hepatic tumors. Am J Roentgenol 177:799-805

Taylor KJ, Ramos I, Morse SS et al (1987) Focal liver masses: differential diagnosis with pulsed Doppler US. Radiology 164:643-647

Van Leeuwen MS, Noordzij J, Feldberg MA et al (1996) Focal liver lesions: characterization with triphasic spiral CT. Radiology 201:327-336

Vilgrain V, Boulos L, Vullierme MP et al (2000) Imaging of atypical hemangiomas of the liver with pathologic correlation. Radiographics 20:379-397

Vilgrain V, Uzan F, Brancatelli G et al (2003) Prevalence of hepatic hemangioma in patients with focal nodular hyperplasia: MR imaging analysis. Radiology 229:75-79

Von Herbay A, Vogt C, Häussinger D (2002) Late-phase pulse-inversion sonography using the contrast agent levovist: differentiation between benign and malignant focal lesions of the liver. Am J Roentgenol 179:1273-1279

Von Herbay A, Vogt C, Willers R, Haussinger D (2004b) Real time imaging with the sonographic contrast agent SonoVue: Differentiation between benign and malignant hepatic lesions. J Ultrasound Med 23(12):1557–1568

Von Herbay A, Vogt C, Haussinger D (2004a) Differentiation between benign and malignant hepatic lesions: Utility of color stimulated acoustic emission with the microbubble contrast agent levovist. J Ultrasound Med 23(2):207–215

Wang JH, Lu SN, Changchien CS, Huang WS et al (2003) Flash-echo gray-scale imaging in the subtraction mode for assessing perfusion of small hepatocellular carcinoma. J Clin Ultrasound 31:451-456

Wang LY, Wang JH, Lin ZY et al (1997) Hepatic focal nodular hyperplasia: findings on color Doppler ultrasound. Abdom Imaging 22:178-181

Wanless IR, Mawdsley C, Adams R (1985) On the pathogenesis of focal nodular hyperplasia of the liver. Hepatology 5:1194-1200

Wang LY, Wang JH, Lin ZY et al (1997) Hepatic focal nodular hyperplasia: findings on color Doppler ultrasound. Abdom Imaging 22:178-181

Ward B, Baker AC, Humphrey WF (1997) Nonlinear propagation applied to the improvement of resolution in diagnostic medical ultrasound. J Acoust Soc Am 101:143-154

Welch TJ, Sheedy PF, Johnson CM et al (1985) Radiologic characteristics of benign liver tumors: focal nodular hyperplasia and hepatic adenoma. Radiographics 5:673-682

Wen YL, Kudo M, Zheng RQ et al (2004) Characterization of hepatic tumors: value of contrast-enhanced coded phase-inversion harmonic angio. Am J Roentgenology 182:1019-1026

Wilson SR, Burns PN, Murdali D et al (2000) Harmonic hepatic ultrasound with microbubble contrast agent: initial experience showing improved characterization of haemangioma, hepatocellular carcinoma and metastasis. Radiology 215:153-161

Yoshikawa J, Matsui O, Takashima T (1988) Fatty metamorphosis in hepatocellular carcinoma: radiological features in 10 cases. AJR Am J Roentgenol 151:717-720